Waun Mawn, Pembrokeshire

Report of Geophysical survey: Frequency Domain Electromagnetic prospection in March 2018.

Site Summary

Monument No(s): RCAHMW 1925: 258-9

Study Area: Waun Mawn, Pembrokeshire

Map reference number: SN08353405

Geophysical survey type: Frequency Domain Electromagnetic Induction (FDEM)

Size of survey area: 5 ha

Geology: gleyed podzol with peat cover, mudstone bedrock

Land use: Agriculture.

Cultivation: Pasture

Field work dates: March 11- 12, 2018

Report: Written by Philippe De Smedt (Ghent University) with Mike Parker Pearson (University College London).

Archive holder: Ghent University and University College London

Technical Details

Technical details

Type of Survey: frequency domain electromagnetics (FDEM), *also referred to as electromagnetic induction (EMI)*

Area Surveyed: 4.8 ha

Traverse Separation: 1.0 m

Sampling Interval: 10 Hz

Instrumentation: Dualem 21HS, Dualem inc., Ontario, Canada.

Introduction

This report outlines the results of the frequency domain electromagnetic induction (FDEM) surveys undertaken in March 2018 in the area surrounding the Waun Mawn Standing Stones (Fig. 1). These surveys were organised by University College London's Institute of Archaeology in conjunction with Ghent University, and formed a fieldwork element of the Stones of Stonehenge project. Within three smaller zones, a total area of 4.8 hectares was surveyed with FDEM. These zones are indicated in the inset on Fig. 1, with red polygons. The area is covered with a peat layer, formed over gleyed podzol soils that developed in loamy sediments. These overlay glacial till and mudstone bedrock (Burt, et al. 2012).

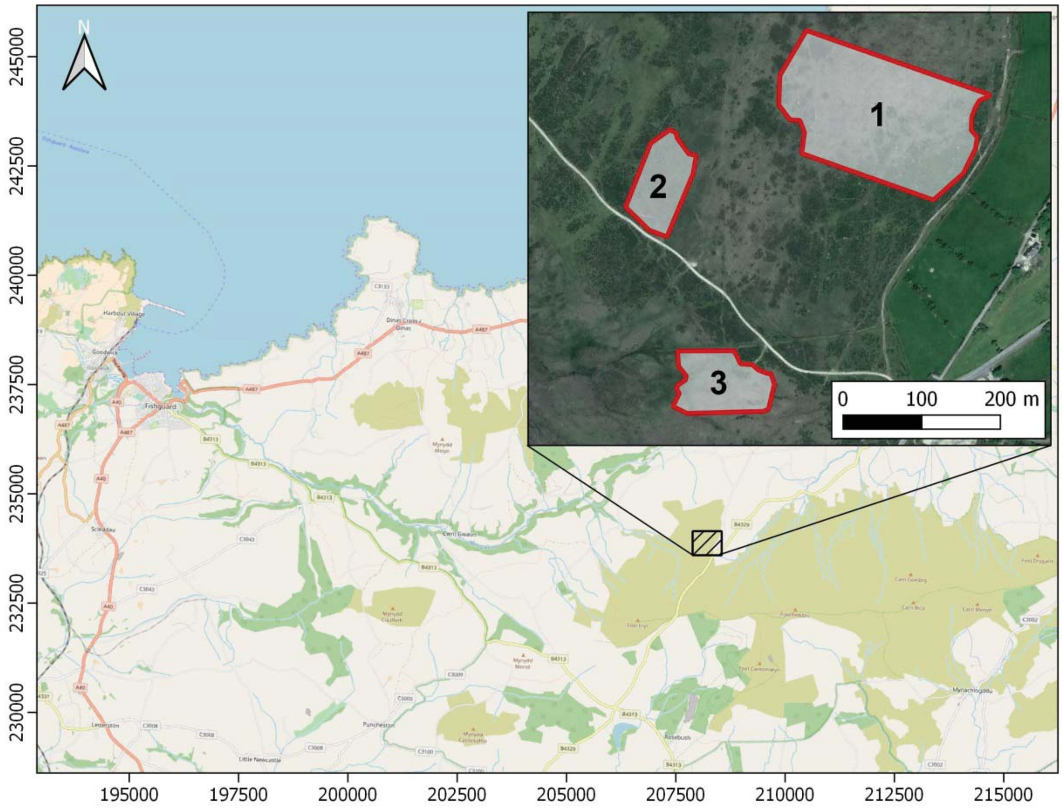

Fig. 1: Study area (hashed bounding box) indicated on the topographical map of the wider area. The inset shows a satellite image of the study area, whereby the surveyed zones (1 – 3) are indicated by red polygons. (Satellite imagery: © 2018 Bluesky Infoterra Ltd & COWI A/S DigitalGlobe Getmapping, and Google; Map data: © 2018 OpenStreetMap)

The overall aim of the FDEM surveys was to collect detailed information on natural soil variations and to offer different physical perspectives (electrical and magnetic) on the (past and (sub-)recent) anthropogenic soil alterations, thereby potentially informing on known and unknown archaeology.

Surveys were conducted on March 11 – 12, under wet soil conditions (near to/fully water saturated soil).

Method

FDEM SURVEY

Multi-receiver FDEM survey was conducted in a mobile manner (Fig. 2). Hereby, a Dualem 21HS sensor was used. This instrument combines one transmitting coil with six receiver coils alternately paired in perpendicular (PRP) and horizontal coplanar (HCP) geometry with the transmitter. These receiving coils are placed at 0.5 m (HCPH), 0.6 m (PRPH), 1 m (HCP1), 1.1 m (PRP1), 2 m (HCP2) and 2.1 m (PRP2) from the transmitter coil. The combination of these differing coil geometries with varying inter-coil separation allows geometric sounding of the survey area. As both the in-phase and out-of-phase component of the FDEM response are recorded, the in-phase magnetic susceptibility (IP_MS) and quadrature phase apparent electrical conductivity (ECa) can be evaluated with each coil pair. Consequently, the Dualem-21HS instrument records both the magnetic and electrical properties of four soil volumes simultaneously. Using the LIN approximate approach (McNeill 1980) to describe considered soil volumes, the instrument effectively allows soil volumes ranging between 0.3 to 3 m beneath the sensor to be considered. The in-phase magnetic susceptibility data are presented in response intensity and expressed in parts per thousand (ppt), unless stated otherwise. As measurements were conducted in non-saline conditions, no corrections other that standard processing procedures (cf. infra) were applied on the IP_MS data. For reference, all raw data are presented in the appendix (Appendix I: A1 - A12).

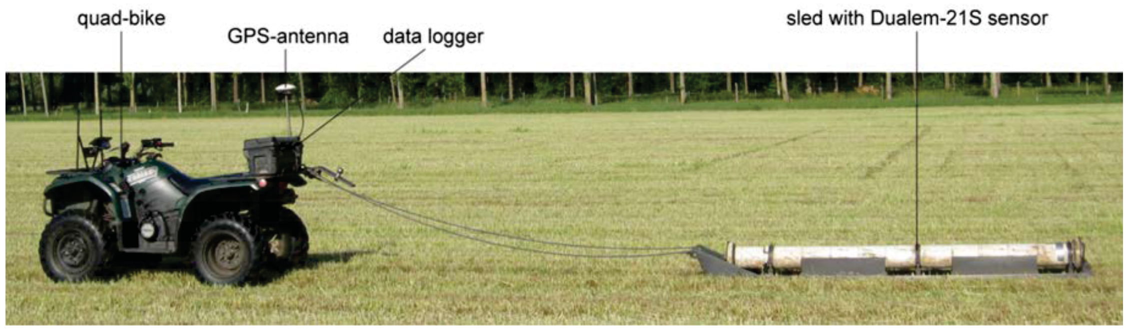

Fig. 2: Mobile survey configuration with the sled-mounted Dualem-21HS towed by quad-bike with data logger and GPS antenna (From De Smedt et al. (2013a))

The Dualem-21HS instrument (Dualem/Geosensors, CA) is placed in a polyethylene sled and towed behind a small all-terrain vehicle (quad bike) (Fig. 2). A fine sampling resolution was chosen to allow:

a) creation of a high resolution map of the natural soil variation and geomorphological features present within the area that can be discriminated through their electrical conductivity or magnetic susceptibility;

b) detection and recording of archaeological features (minimum diameter larger than 1 m^2);
c) efficient survey speed (on average 7 ha per day).

Therefore, sampling resolution was set at 1.0 m x ca. 0.3 m. This was upheld by driving across the survey area along parallel lines in snake-line traverse, 1.0 m apart, at an average speed of 7 km/h while recording at a sampling speed of 10 Hz. At the end of each survey day, calibration data were collected to compensate for measurement drift following Delefortrie et al. (2014). Measurements were georeferenced on-the-go in WGS84 coordinates, and converted to OSGB1936 (BNG – EPSG: 27700) using the Ordnance Survey National Grid Transformation (OSTN02, © Ordnance Survey, 2018). All data and coordinates presented in this report and provided as digital addenda are in OSGB1936.

All data were processed using in-house developed software, following Delefortrie et al. (2014) and Delefortrie et al. (2016). Data interpolation to a 0.25 by 0.25 m grid was performed through nearest neighbour interpolation. Where appropriate, data were high-pass filtered by removing the median within a 10 m diameter circular search window.

The recorded variables (ECa and IP_MS) and influencing subsurface parameters, i.e. the soil electrical conductivity and its magnetic susceptibility relate to different aspects of the subsurface.

Electrical conductivity: in non-saline environments, this moisture-dependent soil property is influenced primarily by soil textural variations (i.e. clay content). Based on what is known about the geology of the environment, ECa is expected to mainly relate to changes in the thickness of the peat layer and underlying soil thickness and the associated till and bedrock depth. Any modification to the upper soil layers (e.g. in the form of ditches and pits) would equally influence the recorded ECa.

Magnetic susceptibility: primarily related to the presence of iron oxides in soil. The study area consists of a complex magnetic soil environment, whereby both the presence of igneous rock fragments and iron panning can render strong magnetic contrasts, burdening the discrimination of more discrete (archaeological) soil modifications. However, it can be hypothesised that local disturbances ferrous soil horizons render strong magnetic contrasts.

Following the expected good correlation between electrical and magnetic properties and the natural geological variation, both parameters inform on the pedological and geomorphological properties of the area.

BOREHOLE SURVEY AND GEOPHYSICAL SOUNDING

To complement the geophysical survey data, downhole electrical conductivity and magnetic susceptibility sounding was conducted. In addition, one reference magnetic susceptibility profile was recorded. In addition, one magnetic susceptibility profile was recorded along an exposed soil profile directly north of zone 3. Downhole magnetic susceptibility data was collected with a Bartington MS2H probe and MS2 sensor (Bartington Ltd, UK), while downhole electrical conductivity data was collected with an Eijkelkamp EC-probe. For both downhole measurements, a 2.5 cm diameter borehole was prepared with a gouge auger. Along the reference profile, susceptibility data were gathered with an SM30 Kappameter (ZH Instruments, CR).

Results

ELECTRICAL CONDUCTIVITY - OVERVIEW

For what is assumed to be a heterogeneous and electrically conductive environment, the ECa variations recorded over the survey area display a surprisingly narrow range (Table 1; Fig. 3 (left)). Statistics for the raw LIN ECa values from each coil pair from the entire survey area (shown in Fig. 3) are shown in Table 1. While the absolute minima and maxima, most notably for the HCPH and PRPH coil pairs, are influenced heavily by strong conductors (such as small metal objects) the interquartile range (IQR; the difference between Q1 and Q3), along with the median of each ECa data layer are representative for the soil conductivity. The obtained values, with a mean IQR of 0.8, show a range just outside the noise levels of FDEM prospection, and demonstrate a remarkably resistive environment considering the governing physical soil properties (i.e. texture, organic matter and moisture content) within the survey area. When the spatial variation between the different subzones is taken into account, survey zone 1 displays the smallest ECa variation (mean IQR: 0.3 mS/m), while the lowest lying area (survey zone 3) has the largest conductivity variation (mean IQR: 0.9 mS/m).

When considering the small scale variation, the most shallow soil volumes recorded (with the 0.6 m PRP coil configuration, Fig. 3 left and right), show a large spatial heterogeneity. However, the range of this variation is near to the instrument noise levels (IQR of 0.5 for the 0.6 m PRP coil pair ECa data). While the overall environment is electrically resistive, zones 2 and 3 display slightly increased conductivities in the deeper ECa data (see the 2.1 m PRP and 2 m HCP data in Fig. 4 left and right, respectively).

Table 1: descriptive statistics of the LIN ECa data (mS/m) collected within the survey area

parameter	**0.5m_HCP**	**0.6m_PRP**	**1m_HCP**	**1.1m_PRP**	**2m_HCP**	**2.1m_PRP**	***mean***
maximum	11.3	58.0	10.3	12.1	12.7	9.1	19.0
minimum	-63.7	-7.0	-25.0	-15.6	-5.8	-8.0	-21.0
mean	-0.6	1.3	0.7	1.4	1.4	0.4	0.7
median	0.3	1.1	0.5	1.3	1.1	0.1	**0.7**
Q1	-1.4	0.9	0.3	1.1	0.8	-0.2	0.3
Q3	0.5	1.4	0.8	1.5	1.5	0.7	1.1
IQR	1.9	0.5	0.5	0.4	0.8	0.9	**0.8**
SD	1.7	0.7	0.9	0.5	1.2	0.9	1

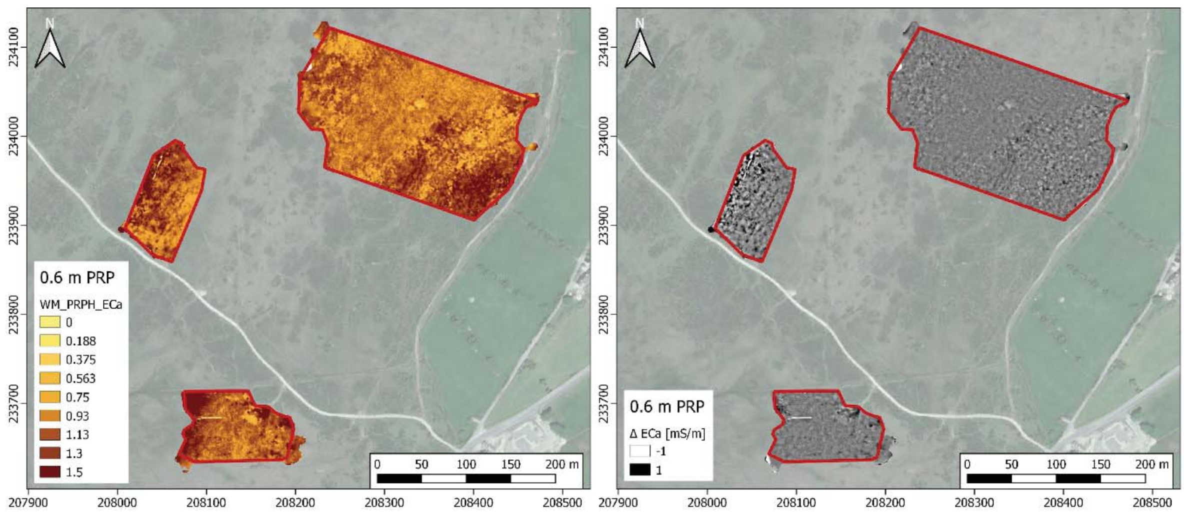

Fig. 3: 0.6 m PRP ECa data (left) and high-passed 0.6 m PRP ECa data (right).

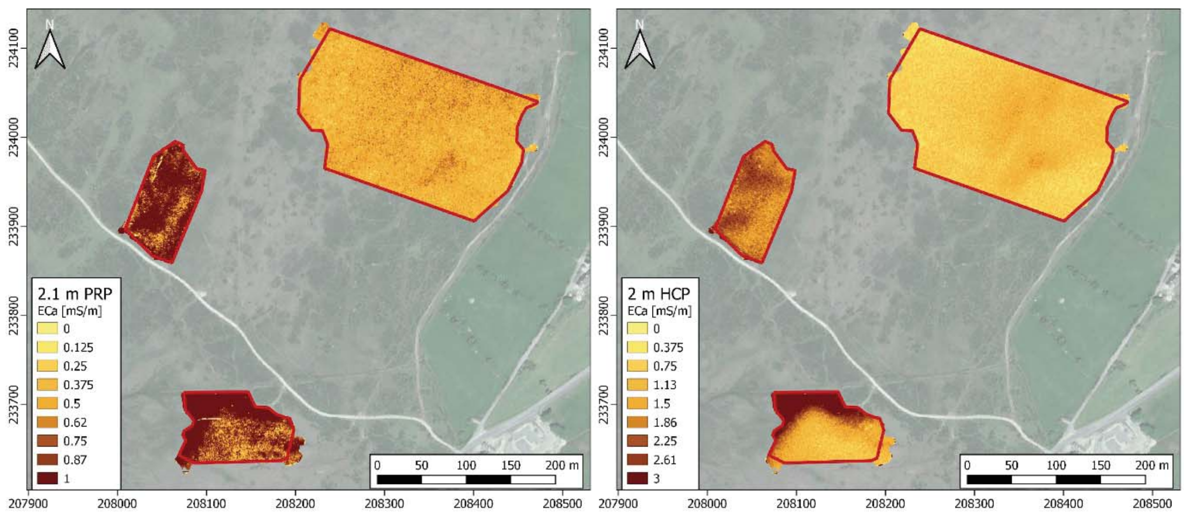

Fig. 4: 2.1 m PRP ECa data (left) and 2 m HCP ECa data (right).

IN-PHASE MAGNETIC SUSCEPTIBILITY – OVERVIEW

Unlike the ECa data, the IP_MS data display a strong variability (Fig. 5). The strongest responses are observed in zones 2 and 3, i.e. in the low-lying parts of the study area. While no absolute MSa data can be derived from the in-phase magnetic susceptibility data without adaptive signal offset correction, the relative MSa values obtained from the 2 m HCP coil pair (representative for the largest soil volume) display a wide range with an IQR of 21.1×10^{-5} for all three survey zones, and 16.7×10^{-5} for survey zone 1 alone.

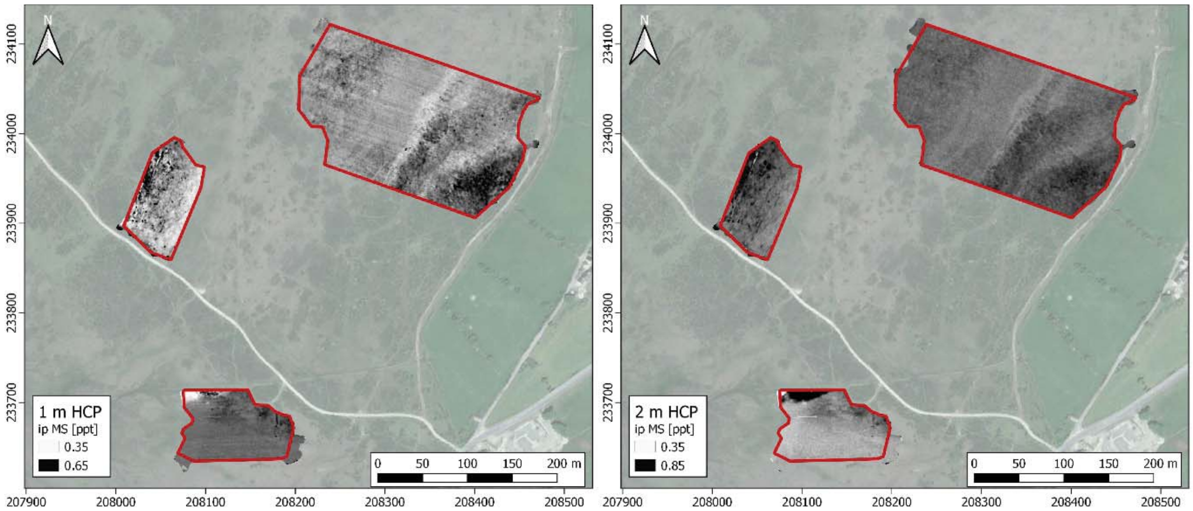

Fig. 5: 1 m HCP in-phase magnetic susceptibility data.

FDEM DATA - INTERPRETATION

The heterogeneous geology of the area is not reflected in the electrical survey data, as the observed poor conductivities render little insight into changes in soil texture, organic matter content of bedrock depth and structure in the area. The slight ECa observed throughout the surveyed areas, particularly in zones 2 and 3, is likely related to the presence of more clayey and/or more organic sediments in the upper 50 cm beneath the surface. In certain areas, the coil pairs which record the largest soil volume indicate subtle increases in soil conductivity. However, considering the amplitude of these responses, which lie within the instrumental noise levels, interpreting this variation is impossible. The characteristic geological variations observed in the FDEM data are indicated on Fig. 6, left. Here, the magnetic variation are interpreted as local occurrences of natural magnetic iron oxides and hydroxides, likely related to iron panning in the podzol soils governing the area. The intermittent spatial spread of magnetic layers in the subsurface relates to spatial variability in the depth, concentration or magnetic properties of these magnetic minerals. This magnetic background variation likely hinders the detection of smaller scale magnetic variations, as it determines the intensity of the contrast possible anthropogenic (archaeological) structures might produce.

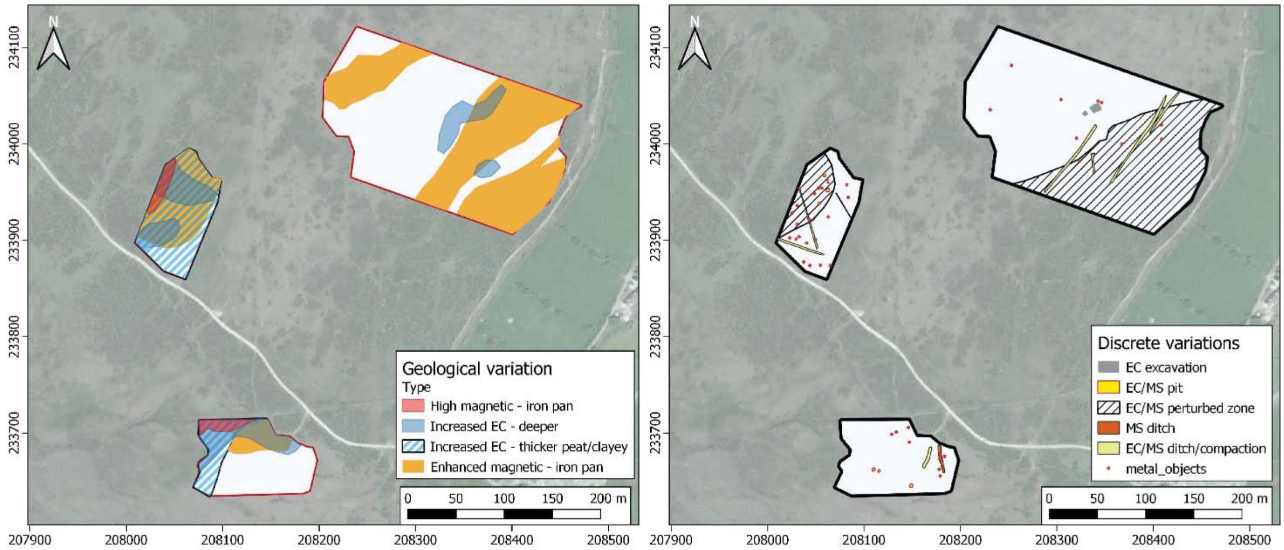

Fig. 6: Geological variation map based on the FDEM data (left), and small scale features detected in the survey data.

The small scale variation that can be observed in the geophysical data indicates little archaeological variation within the survey area. While the data show different linear features (indicated on Fig. 6, left), the nature of the observed responses suggests these are mostly shallow (upper 20 cm) structures of which most are likely related to current trackways. One exception is a possible ditch, filled in with magnetic material in zone 3 (MS ditch on Fig. 6). In zone 2, five large possible pits were attested (Fig. 7). While an archaeological origin cannot be excluded, the geophysical data indicate at least 20 metal objects in zone 2, along with a high concentration of magnetic surface disturbances, hinting at potential recent soil perturbations.

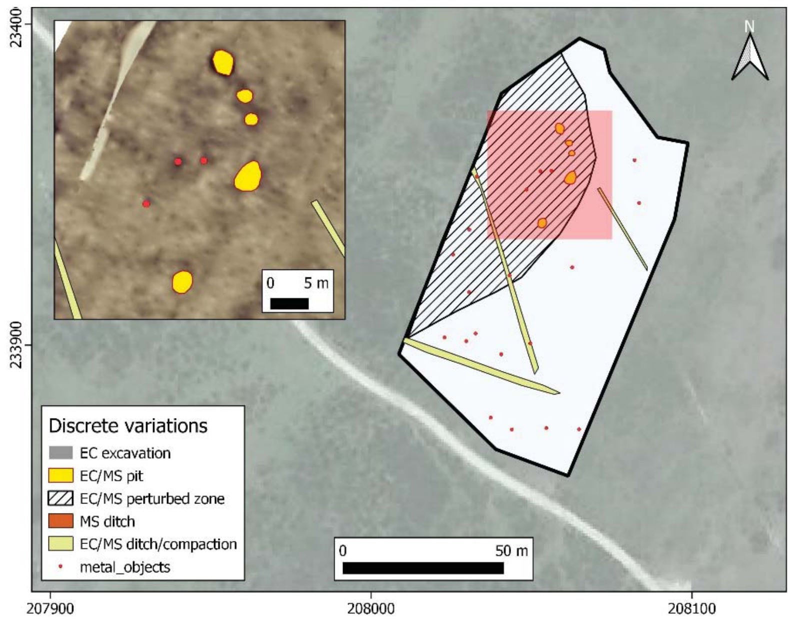

Fig. 7: Small scale variation attested at zone 2, with a detail of the area where different pits were attested (indicated with the red box on the overview image, and shown in the inset).

BOREHOLE SURVEY AND GEOPHYSICAL SOUNDING

To complement the geophysical survey data, downhole electrical conductivity and magnetic susceptibility sounding was conducted at four borehole locations in zone 1 (Fig. 8). At each of these locations, standard soil description was performed as well. In addition, one reference magnetic susceptibility profile was recorded. In addition, one magnetic susceptibility profile was recorded along an exposed soil profile directly north of zone 3 (reference profile on Fig. 8). Downhole magnetic susceptibility data was collected with a Bartington MS2H probe and MS2 sensor (Bartington Ltd, UK), while downhole electrical conductivity data was collected with an Eijkelkamp EC-probe. For both downhole measurements, a 2.5 cm diameter borehole was prepared with a gouge auger. Along the reference profile, susceptibility data were gathered with an SM30 Kappameter (ZH Instruments, CR).

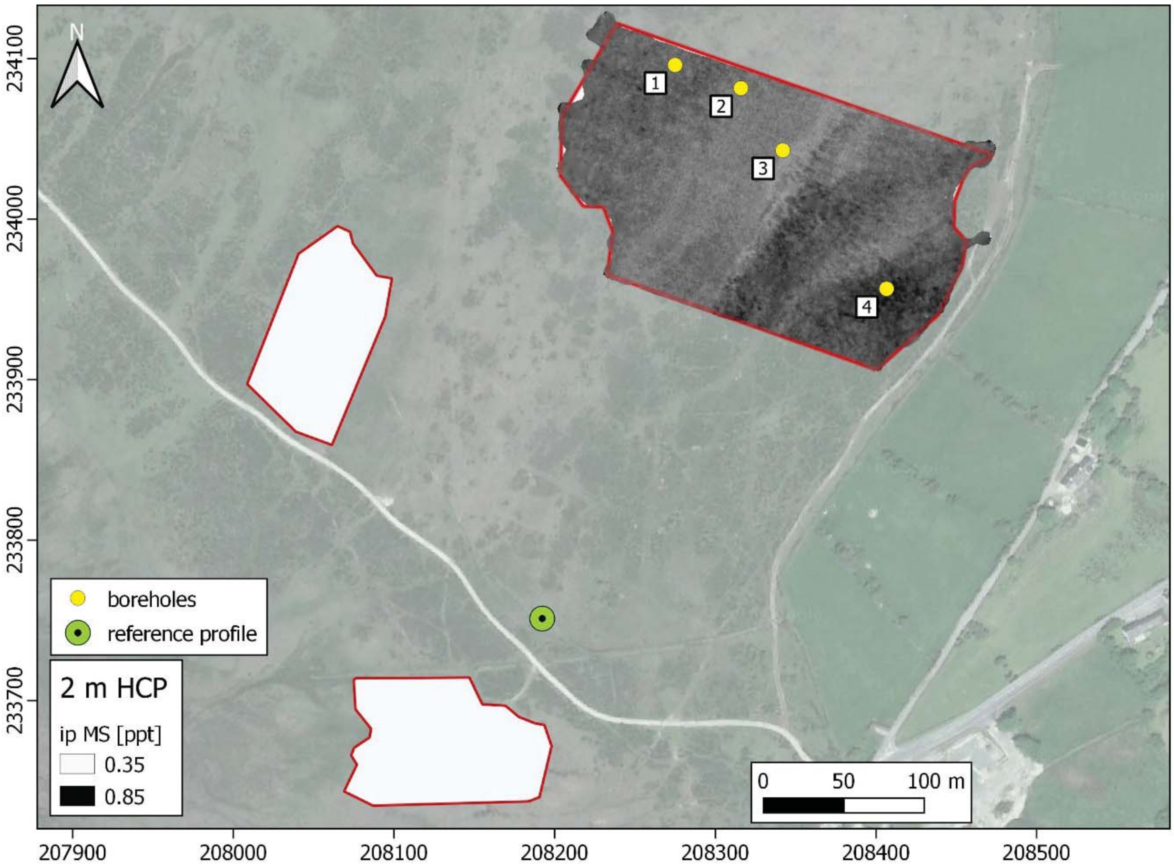

Fig. 8: Location of the four borehole locations within zone 1 plotted on the 2 m HCP IP_MS data, along with the location of the reference profile collected north of zone 3.

At all four borehole locations podzol soils were attested. The most shallow soil profile was observed at borhole 3 (BH 3, Fig. 9), where from -30 cm onwards glacial till extended down to the end of the gouge borehole (-140 cm). While most sampled soil layers consist of material contributing to electrical conductance (finegrained, silty soils; high organic matter content in the upper soil layers; peat O horizon; etc.), the in-situ recorded electrical conductivity data showed the entire environment as strongly resistive. While the O horizons at all locations displayed a maximum of 1.8 mS/m, for all deeper horizons and soil layers, no reliable EC-data could be collected. Here, soil resistivity was too high (>2000 ohms, raw sensor output; i.e. beyond the EC-probe range), resulting in electrical conductivities below 1.3 mS/m. While chemical analysis indicates a lack of ions in the soil solution and absence of charged soil particles. The magnetic susceptibilty profiles at each borehole location show more diversity, confirming the variation observed in the FDEM data.

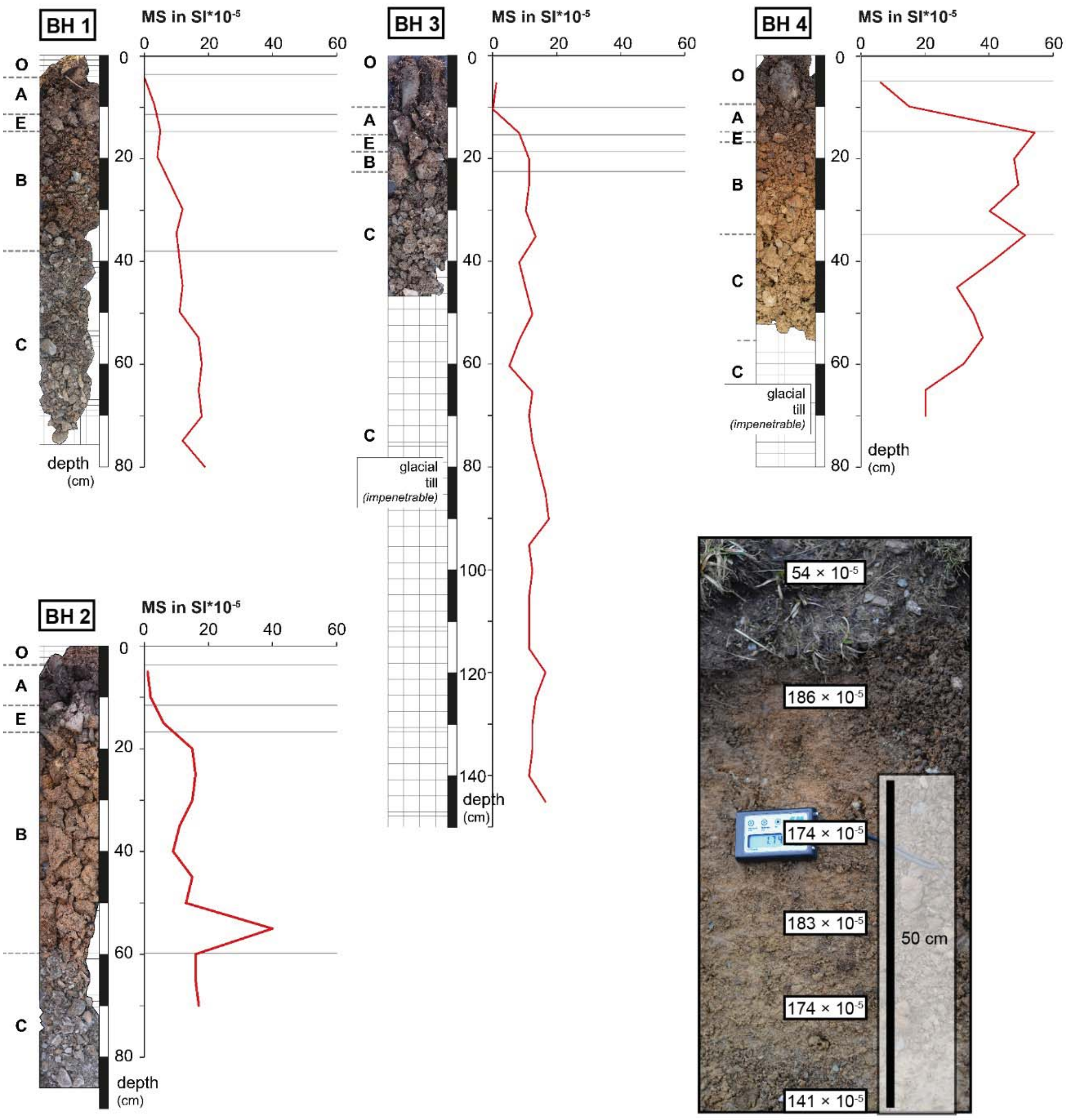

Fig. 9: Photos of the soils sampled at boreholes 1 – 4 (BH1 – 4), with indication of horizonation and the in-situ recorded magnetic susceptibility data. The horizontal lines indicated on the magnetic susceptibility logs indicate the interfaces between the different soil horizons. In the bottom right, the reference profile north of zone 3 is shown, with indication of the magnetic susceptibility values recorded along the profile.

For BH 1 and 3, moderate susceptibilities are recorded, while at BH 2 and BH 4, higher values (maximum of 40.0×10^{-5} and 54.0×10^{-5}) are recorded, coinciding with a clear ferrous Bs horizon. Such an increase in susceptibility is also observed in the reference profile north of zone 3, albeit with much higher absolute values (maximum of 186.0×10^{-5}). The increase in susceptibilty recorded at BH 2 and 4, and along the reference profile, is likely related to magnetic iron oxides and hydroxides. However, the difference in intensity of the magnetic response across the study area is probably due to different redox conditions, stimulating the creation of more magnetic iron oxides and hydroxides particularly in the lower lying areas (e.g. reference profile).

Discussion and conclusion

The electrical and magnetic variation recorded with the FDEM survey, testifies of a complex pedological and geological environment. Electrically, no significant variability was attested in all but the most shallow soil volumes that were recorded (i.e. the 0.5 m HCP and 0.6 m PRP ECa data). The downhole conductivity data, observed in BH 1 – 4, show this absence of contrast and poor signal to noise ratio is a consequence of a highly resistive subsurface. As such, observing any small scale electrical contrast, for instance related to small pits or ditches, with the applied FDEM instrumentation is unlikely. While measurements were performed in water saturated soil conditions, true soil conductivity varied between 0 – 1.8 mS/m, which is a too narrow range to map reliably with FDEM instrumentation. The potential for discerning archaeological features electrically with FDEM instrumentation is therefore poor.

The magnetic contrasts are much stronger. However, as the background magnetic signal varies strongly across the study area – likely a consequence of the different redox conditions across the area – the geological conditions again impede reliable detection of small scale structures or archaeological features.

While potential pit features and indications of soil disturbances were found in zone 2, is not possible to derive clear archaeological information from the current FDEM dataset. The geological characteristics of the study area burden any interpretation, and, particularly for the electrical datasets, the range of variation lies within – or just outside – the instrumental noise levels. Based on the borehole and profile data, and the in-phase FDEM data, it can be assumed that the implementation potential of any magnetic survey technique within the area is limited. Targeting electrical variation likely offers the most potential. Considering the limited range of electrical variation within the survey area, resistance survey might help recording small-scale variations within the resistive environment (0 – 1.8 mS/m) more clearly. In addition, again considering the resistive background, ground penetrating radar survey could equally render positive results, as signal attenuation due to the subsurface conductivity will be negligible. However, any success of a geophysical survey at Waun Mawn hinges on the geophysical contrast possible archaeological structures at the site display against the geological background. Evaluating such contrast was not possible in this study.

References

Burt CE, Aspden JA, Davies JR, Hall M, Schofield DI, Sheppard TH, Waters RA, Wilby PR, Williams M. 2012. Geology of the Fishguard District: a brief explanation of the geological map Sheet 210 Fishguard. Nottingham, UK: British Geological Survey.

Delefortrie S, De Smedt P, Saey T, Van De Vijver E, Van Meirvenne M. 2014. An efficient calibration procedure for correction of drift in EMI survey data. Journal of Applied Geophysics 110(0):115-125.

Delefortrie S, Saey T, De Pue J, Van De Vijver E, De Smedt P, Van Meirvenne M. 2016. Evaluating corrections for a horizontal offset between sensor and position data for surveys on land. Precision Agriculture 17(3):349-364.

McNeill JD. 1980. Electromagnetic terrain conductivity measurement at low induction numbers. Technical Note 6. Ontario: Geonics Limited. 13 p.

Appendix I. Raw data plots

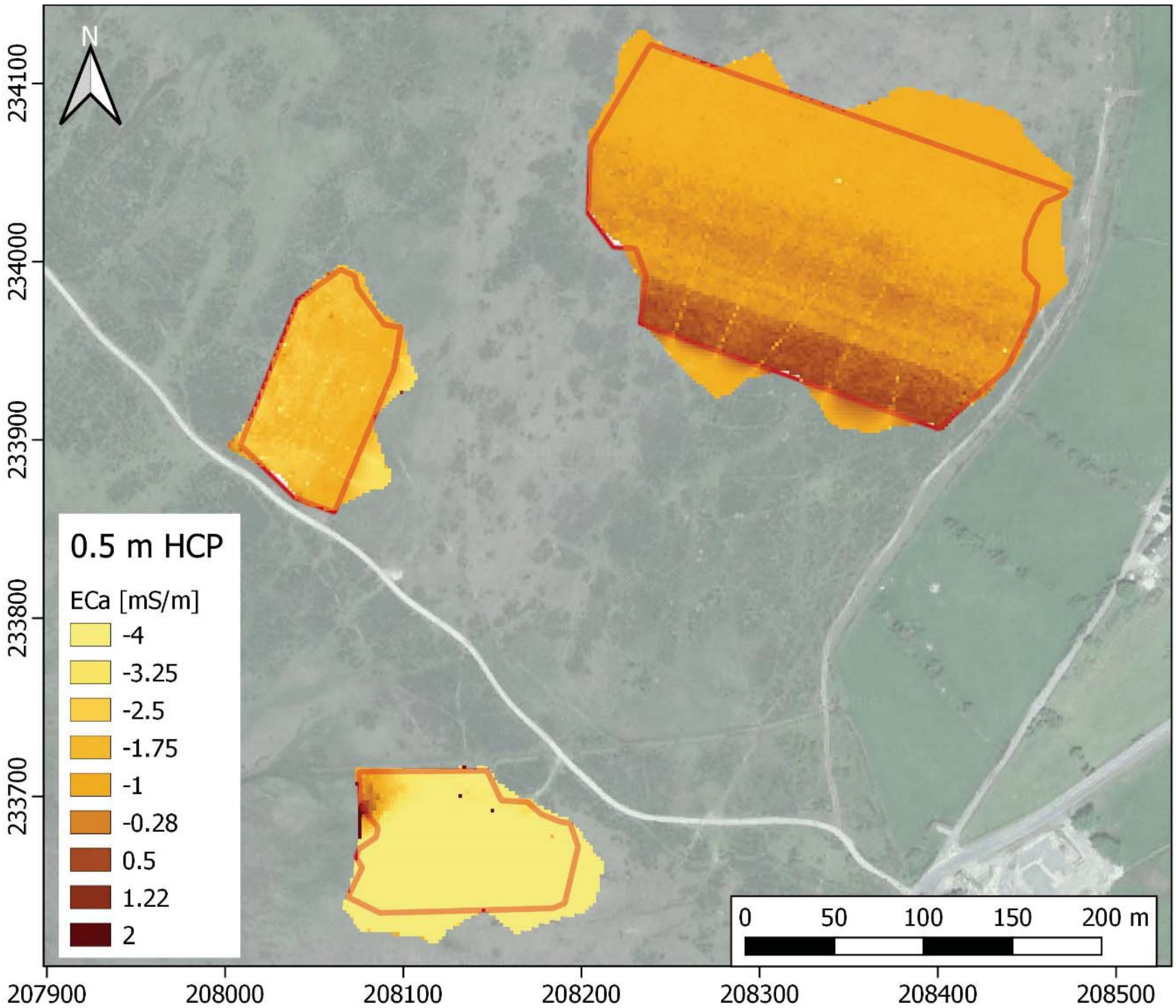

A 1: 0.5 m HCP - raw ECa data.

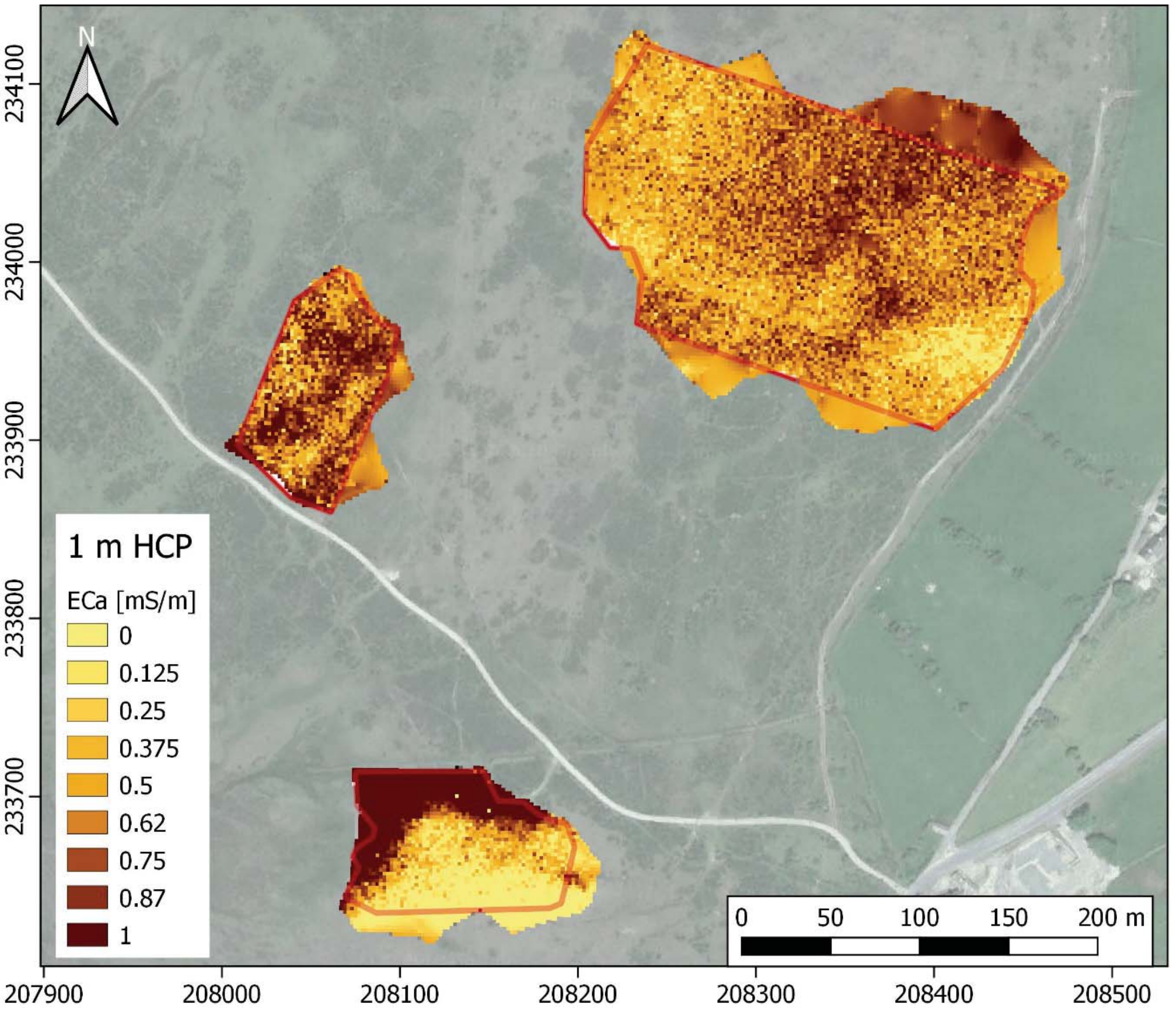

A 2: 1 m HCP - raw ECa data.

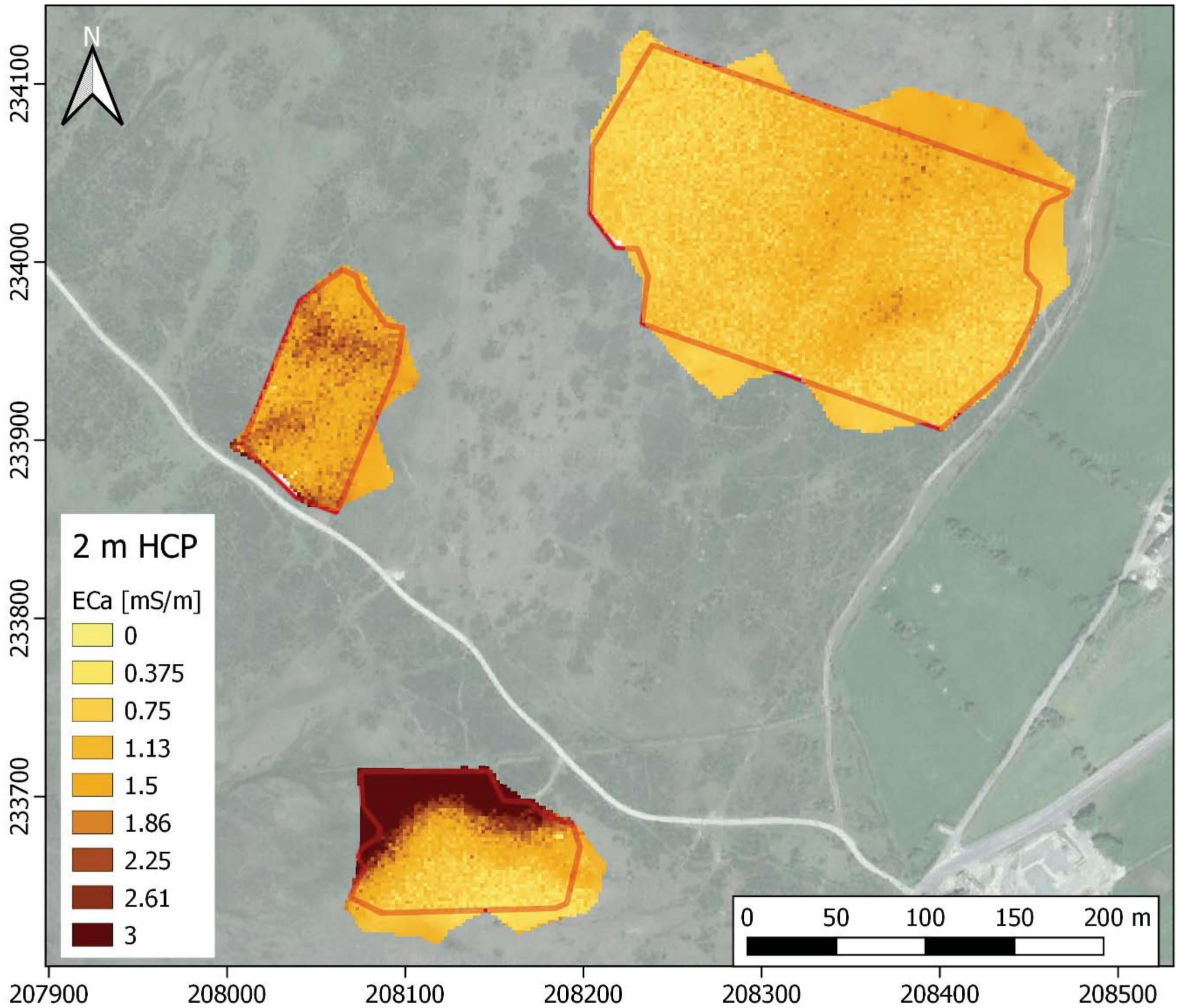

A 3: 2 m HCP - raw ECa data.

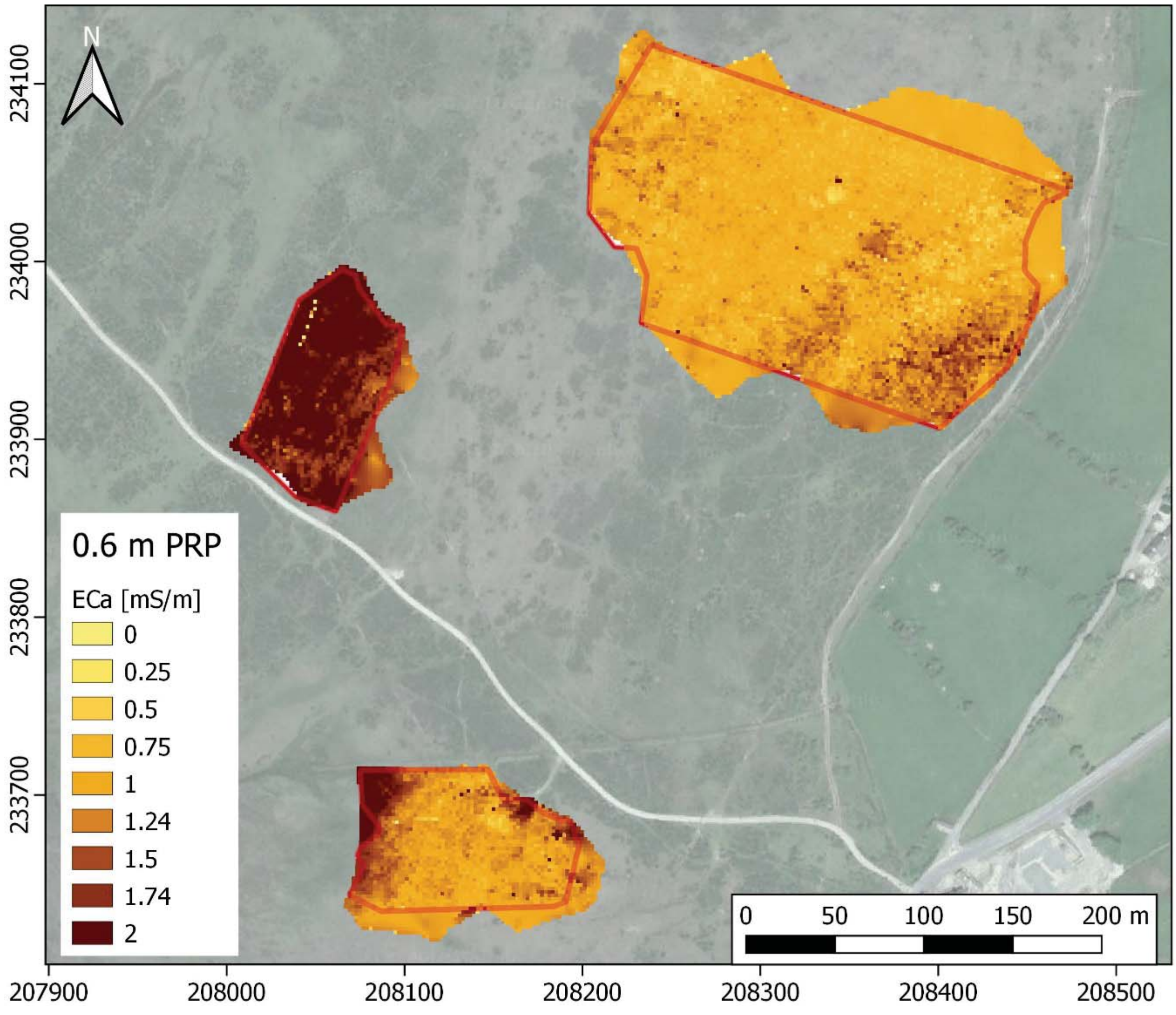

A 4: 0.6 m PRP - raw ECa data.

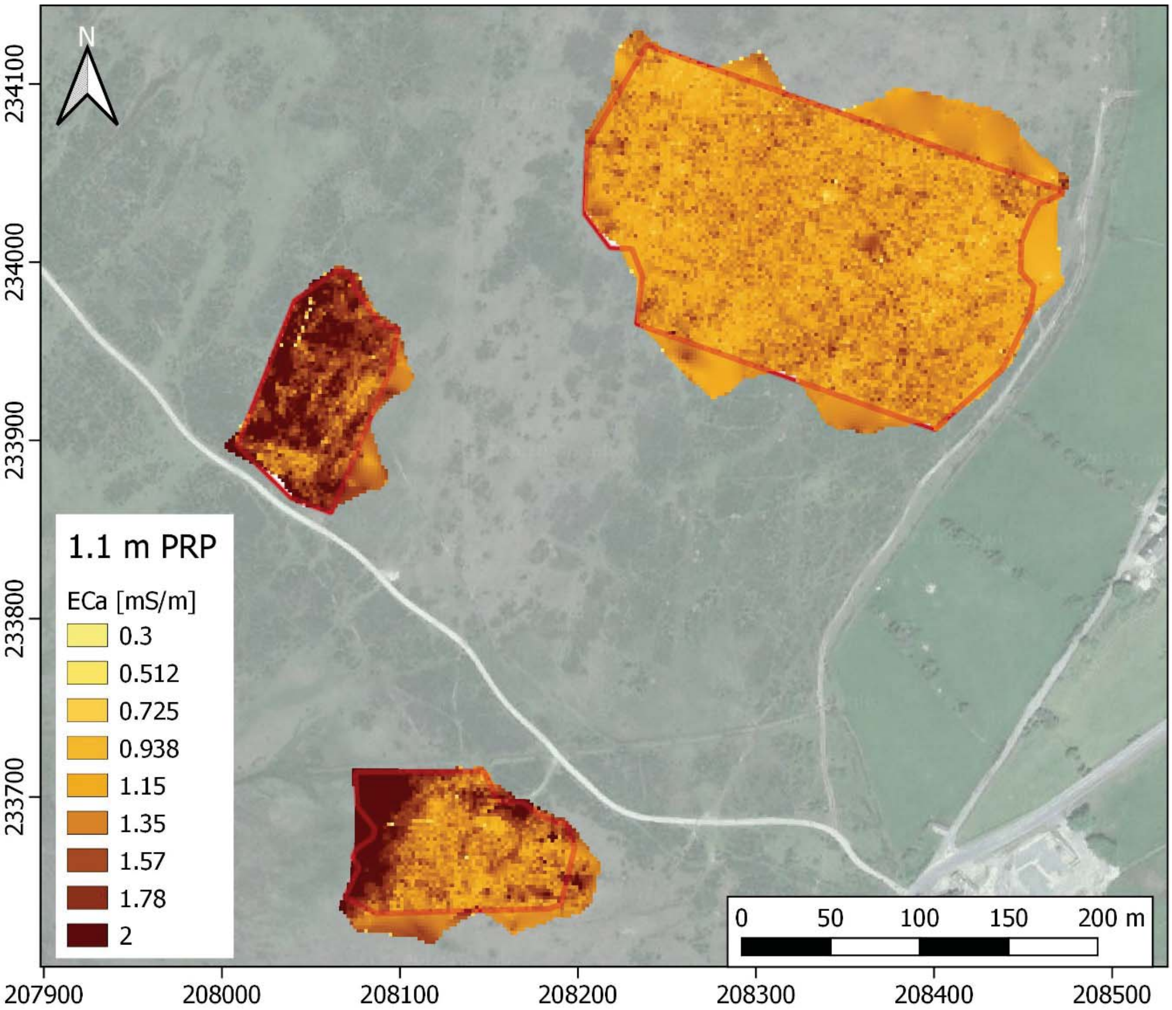

A 5: 1.1 m PRP - raw ECa data.

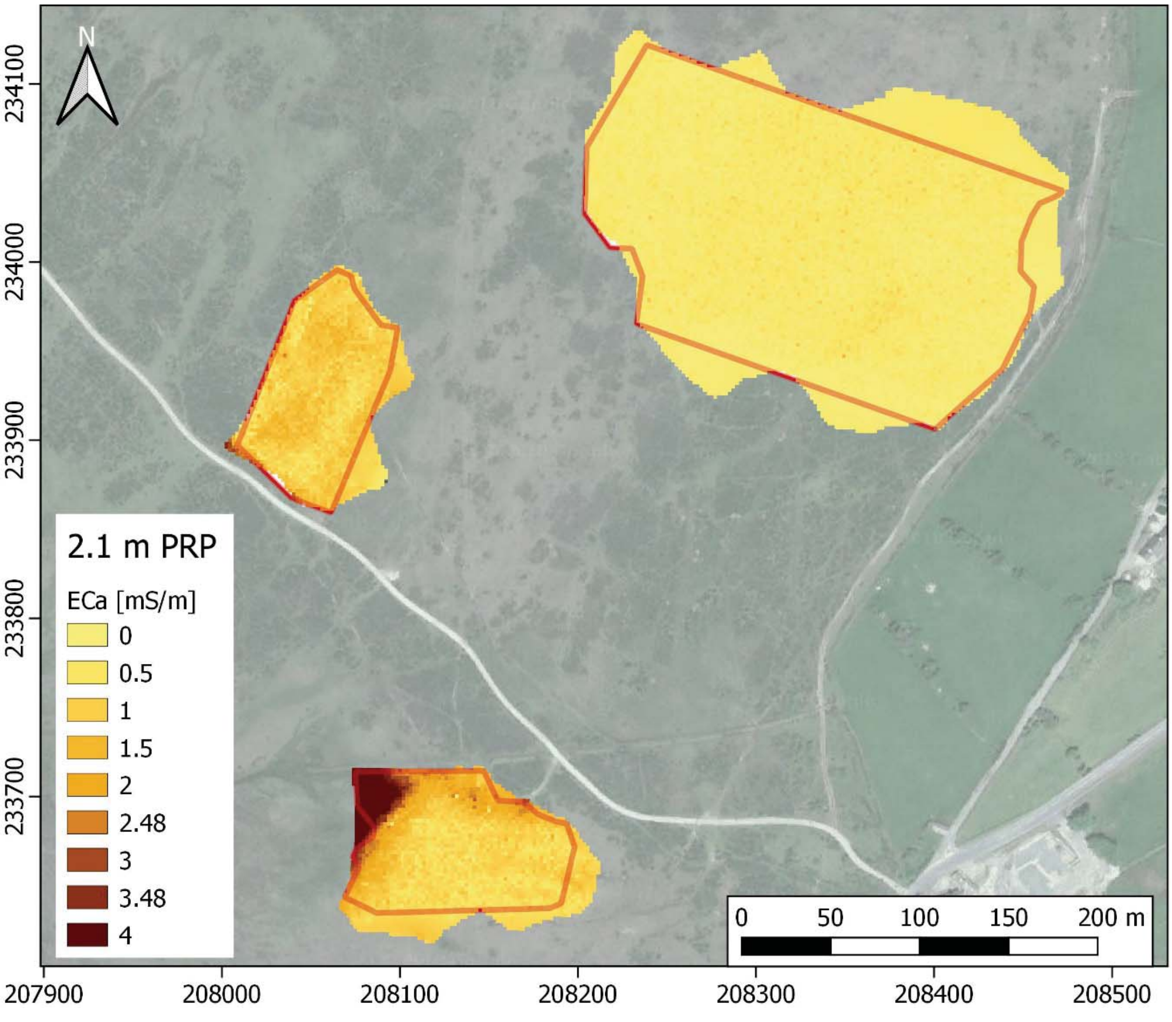

A 6: 2.1 m PRP - raw ECa data.

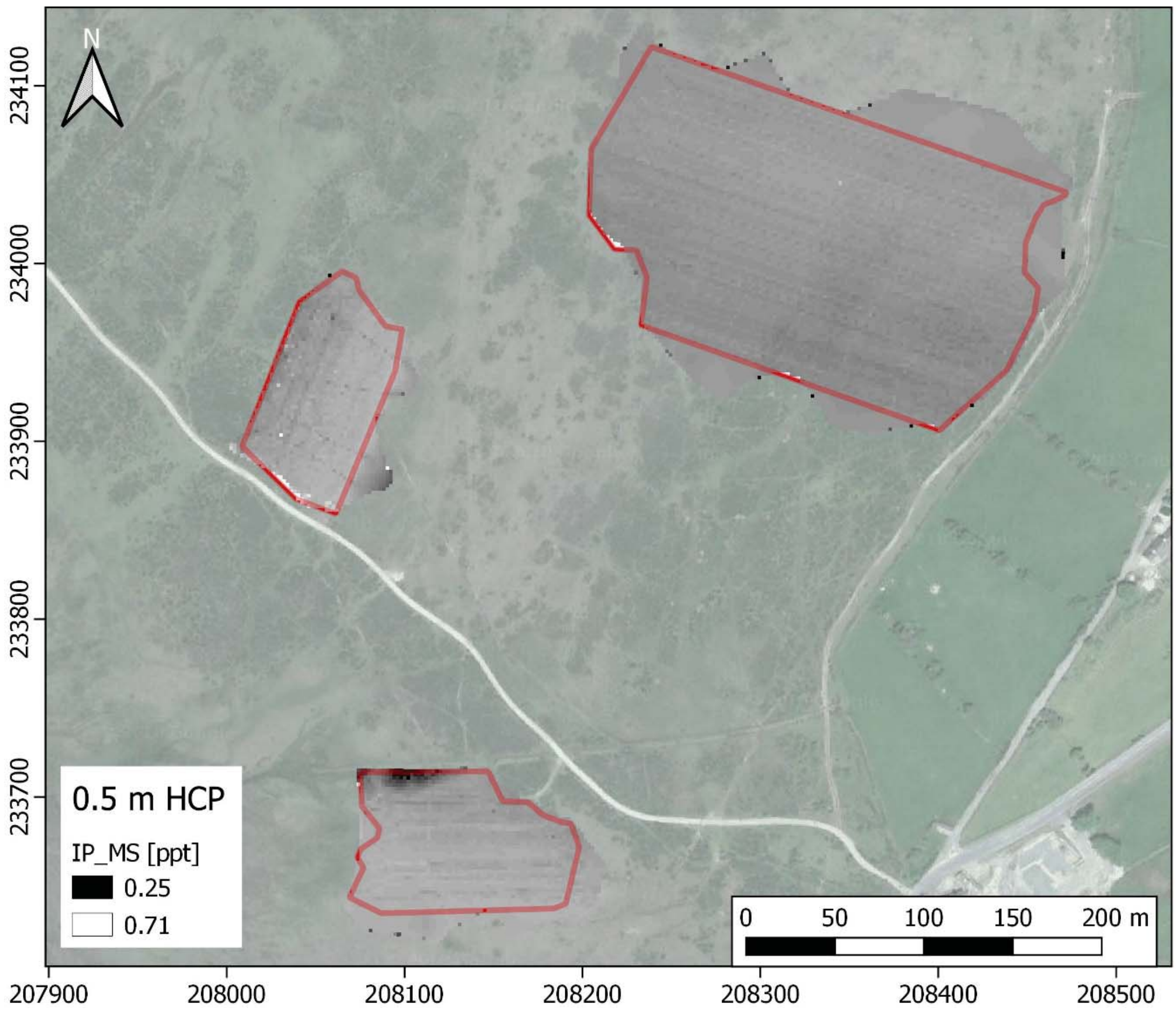

A 7: 0.5 m HCP - raw IP_MS data.

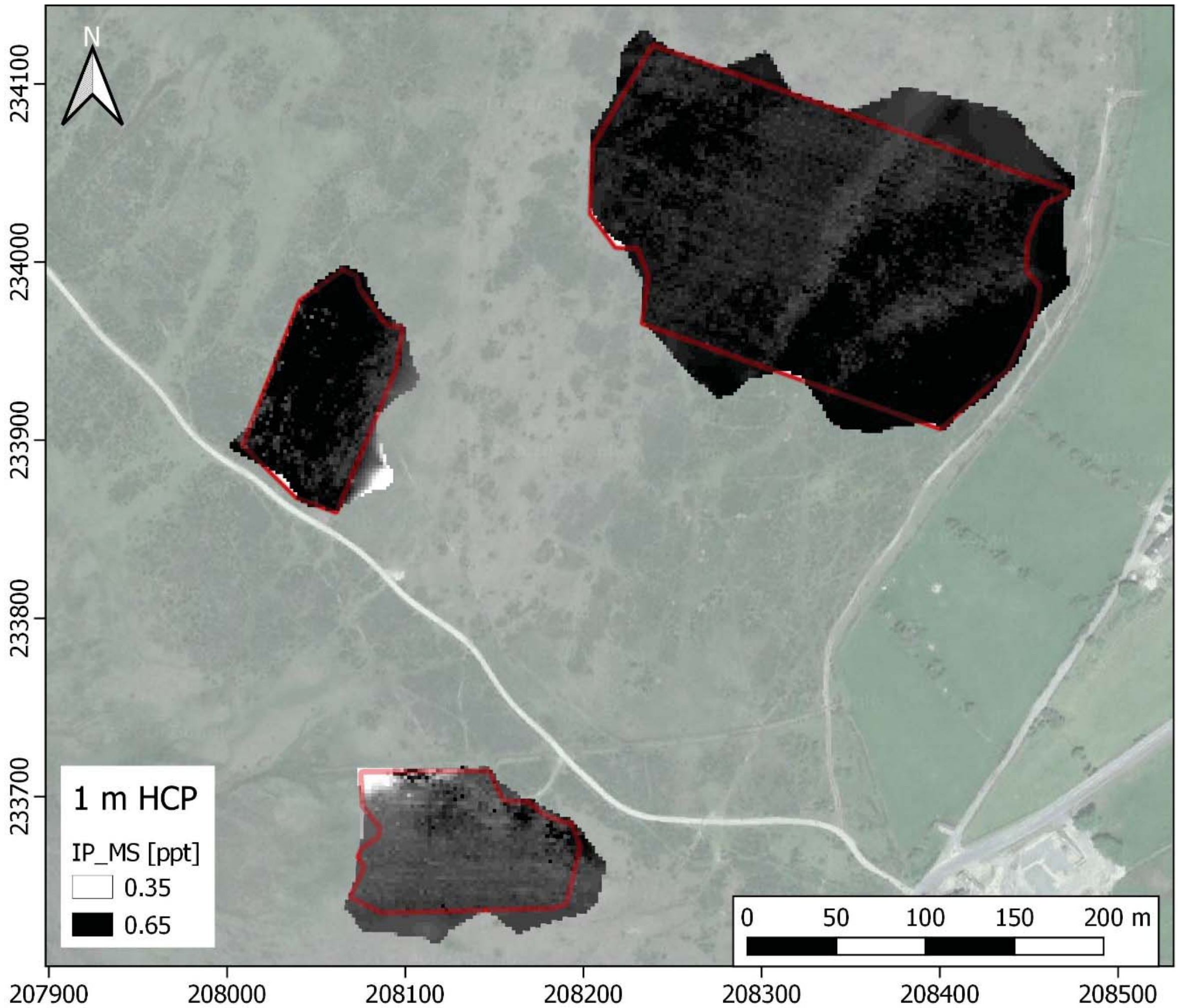

A 8: 1 m HCP - raw IP_MS data.

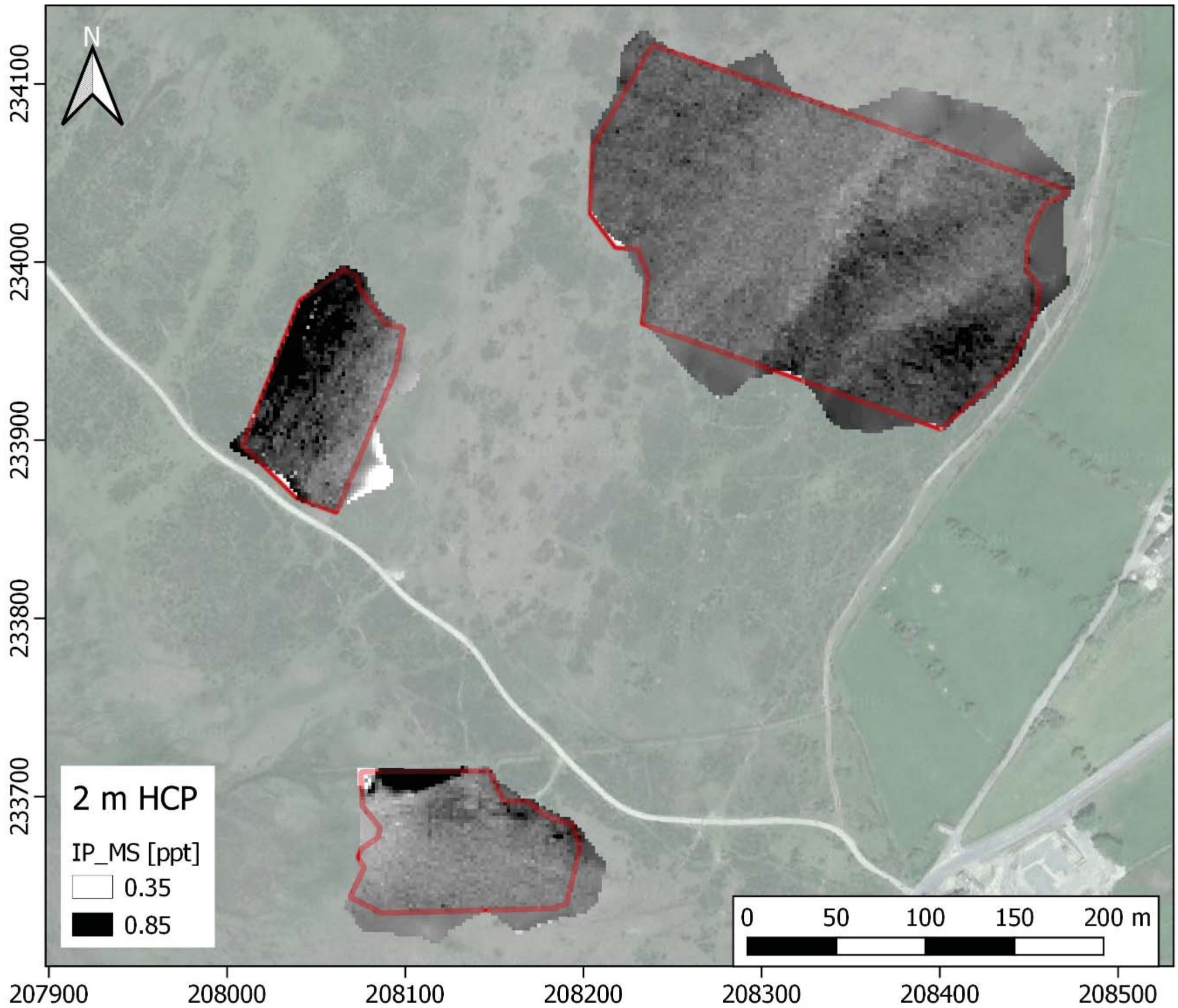

A 9: 2 m HCP - raw IP_MS data.

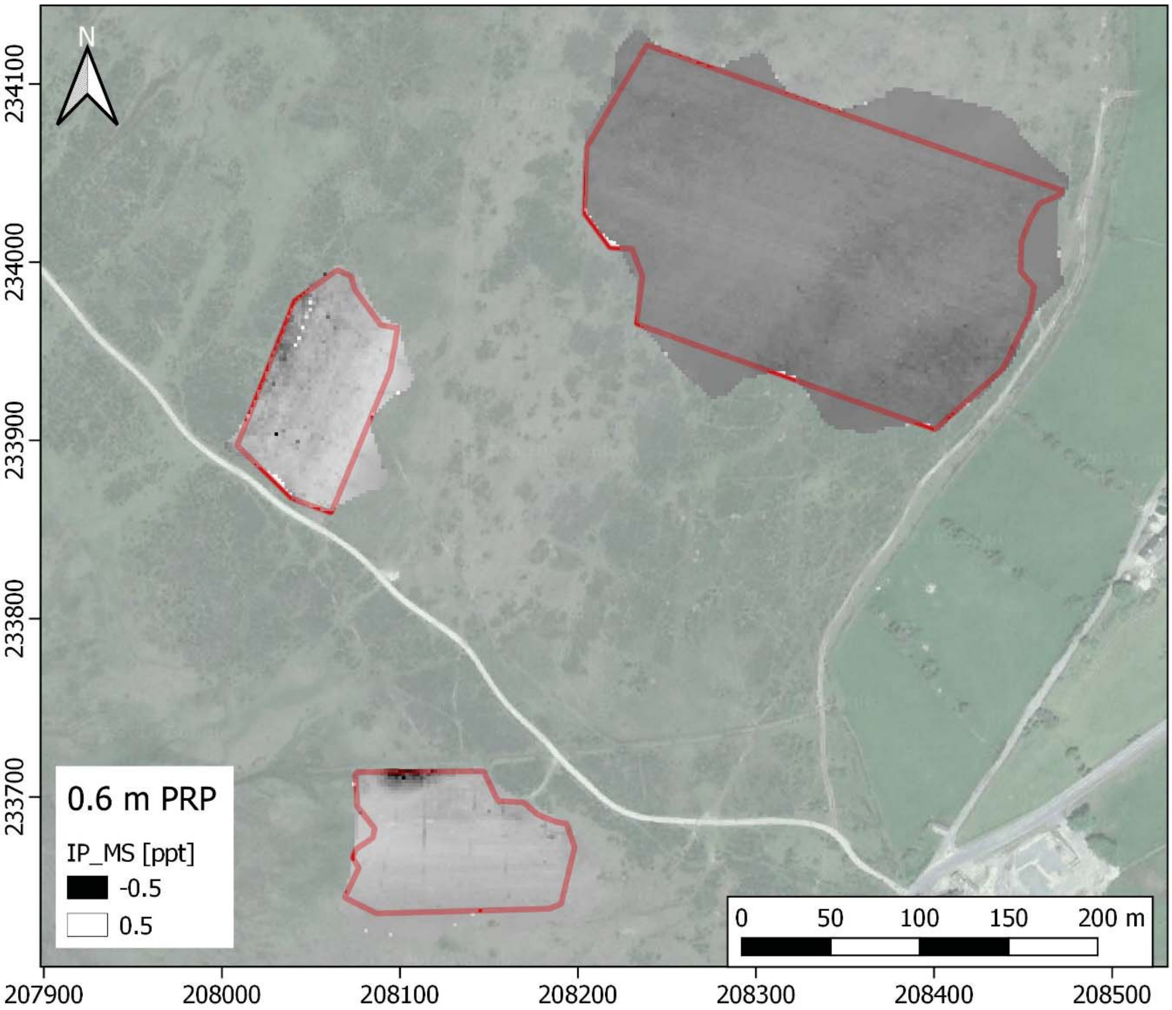

A 10: 0.6 m PRP - raw IP_MS data.

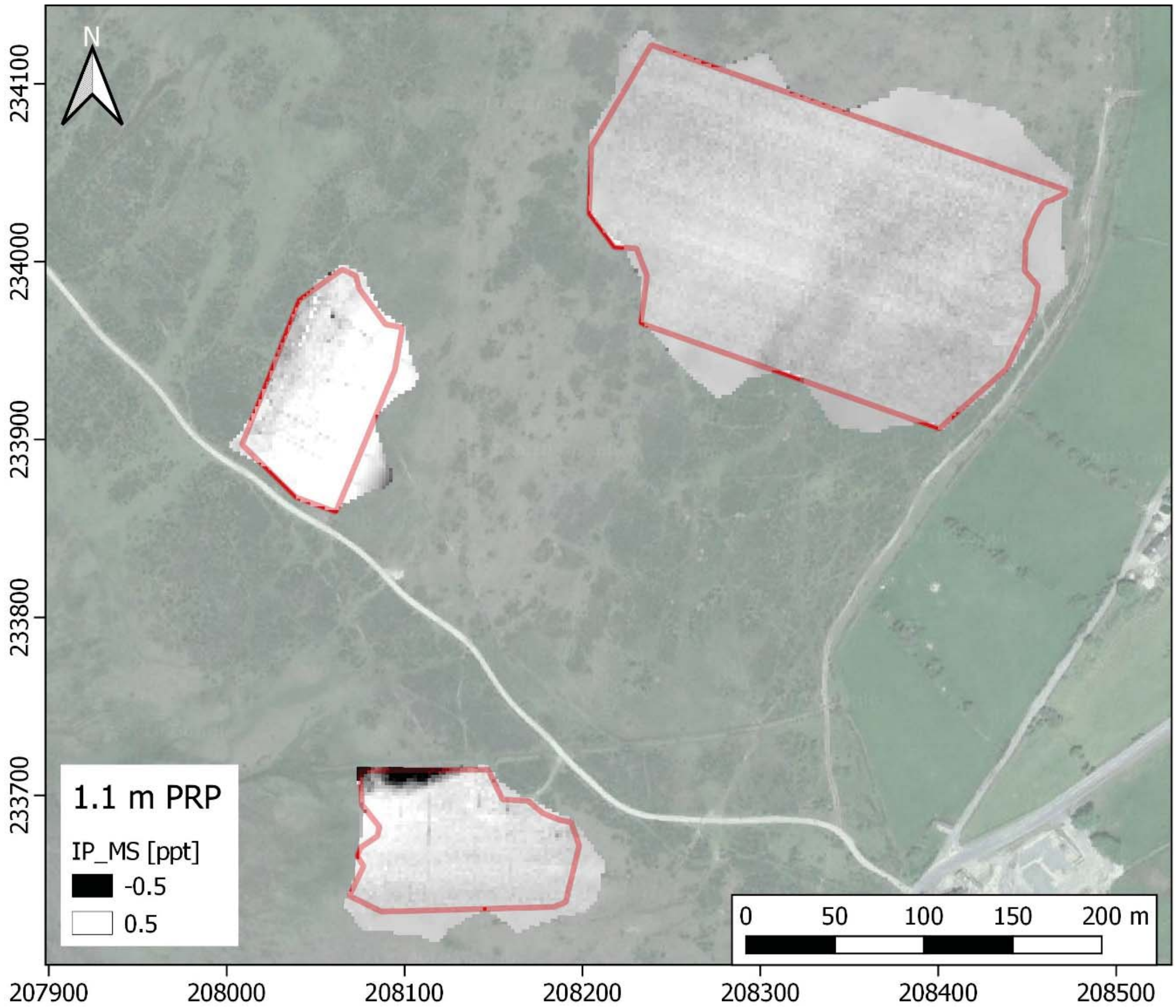

A 11: 1.1 m PRP - raw IP_MS data.

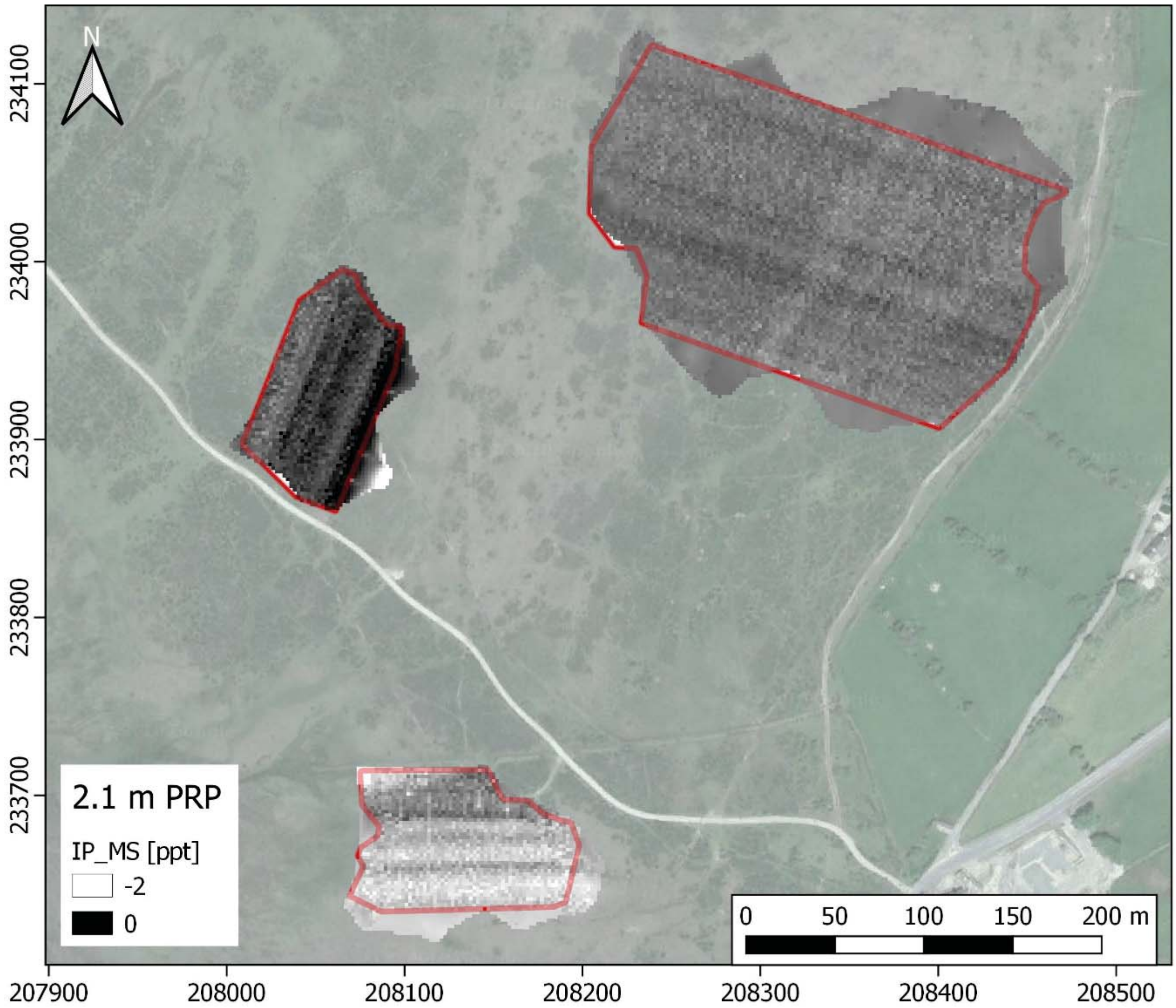

A 12: 2.1 m PRP - raw IP_MS data.

Appendix II. Processed data plots

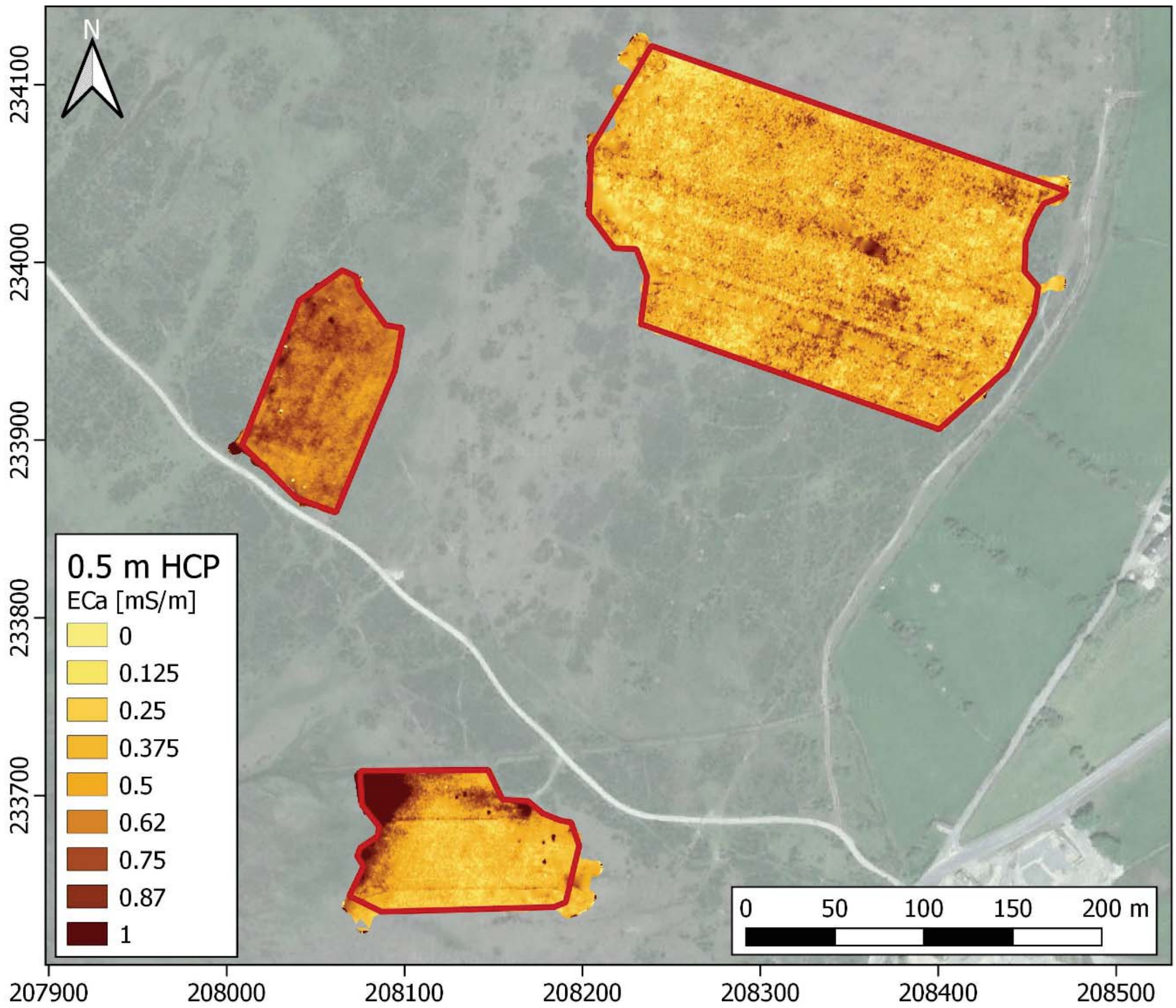

A 13: 0.5 m HCP - ECa data.

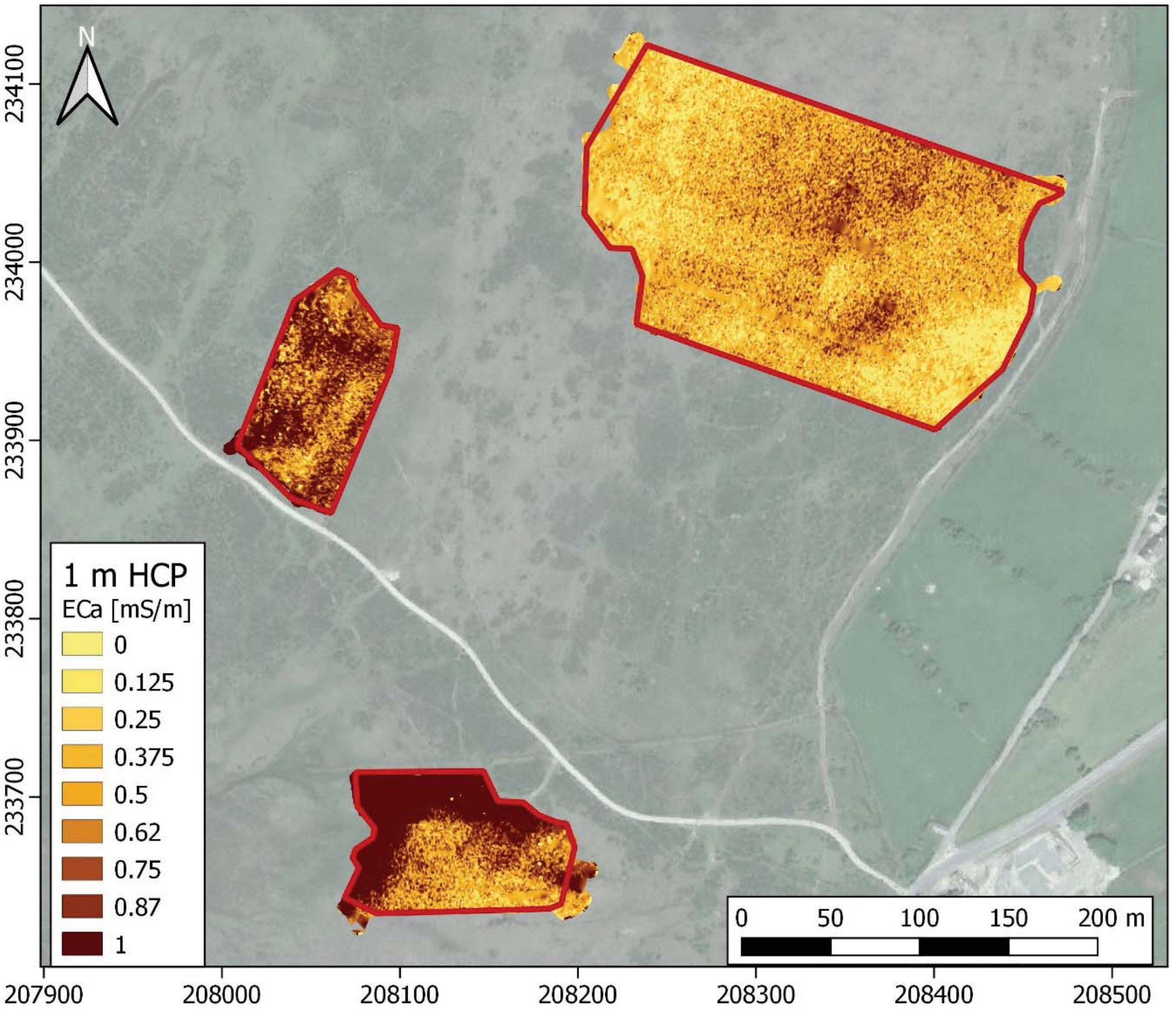

A 14: 1 m HCP - ECa data.

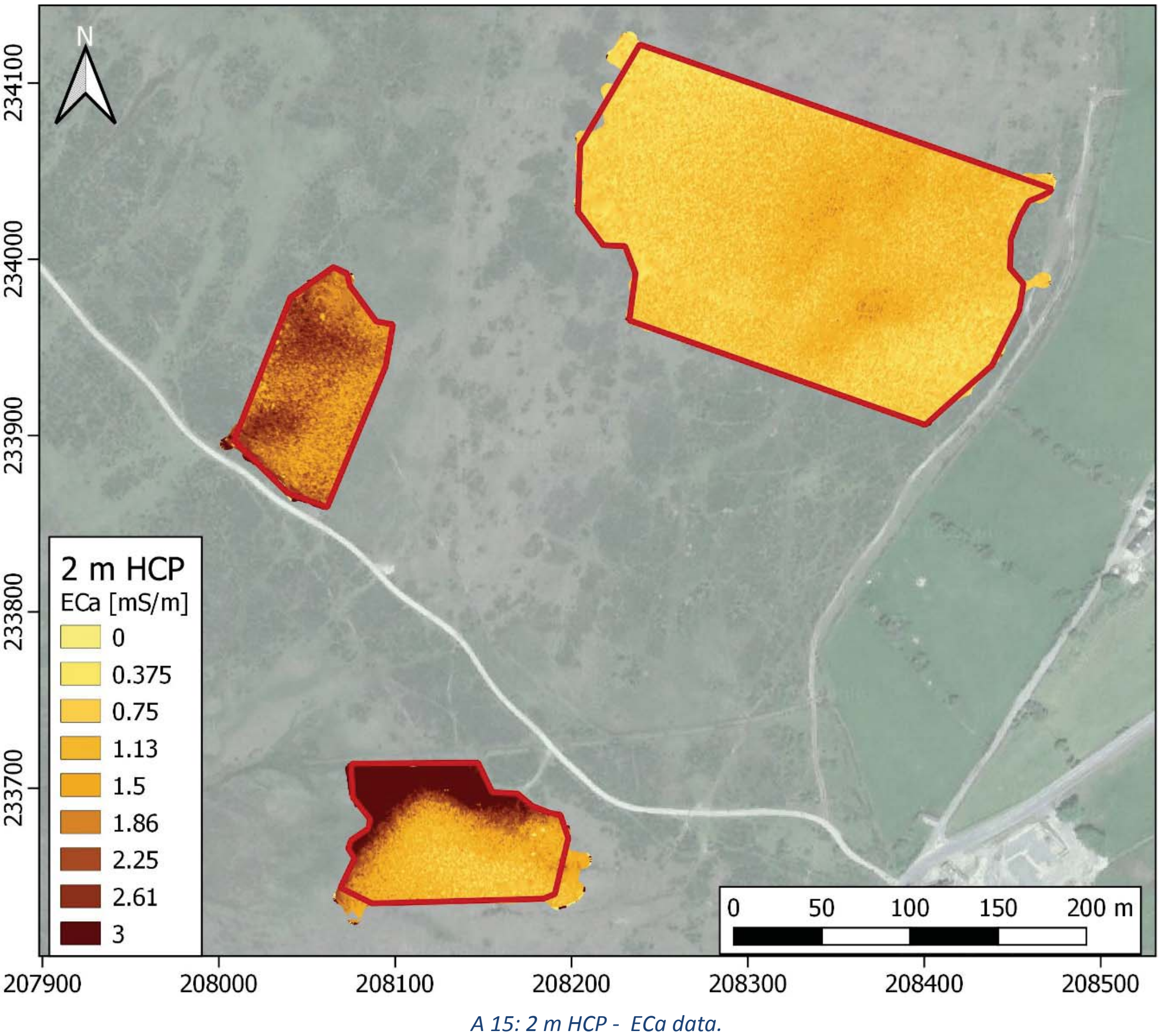

A 15: 2 m HCP - ECa data.

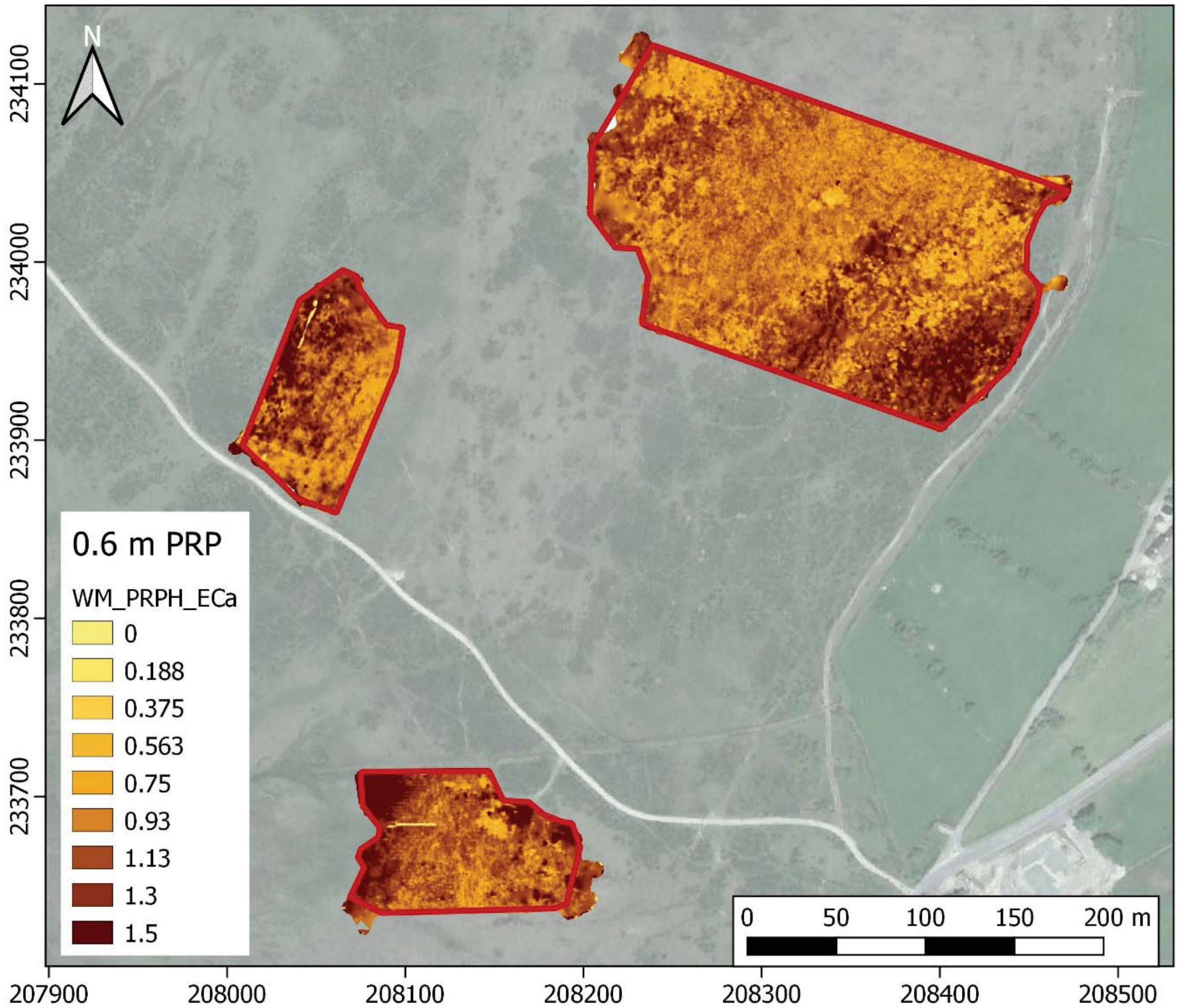

A 16: 0.6 m PRP - ECa data.

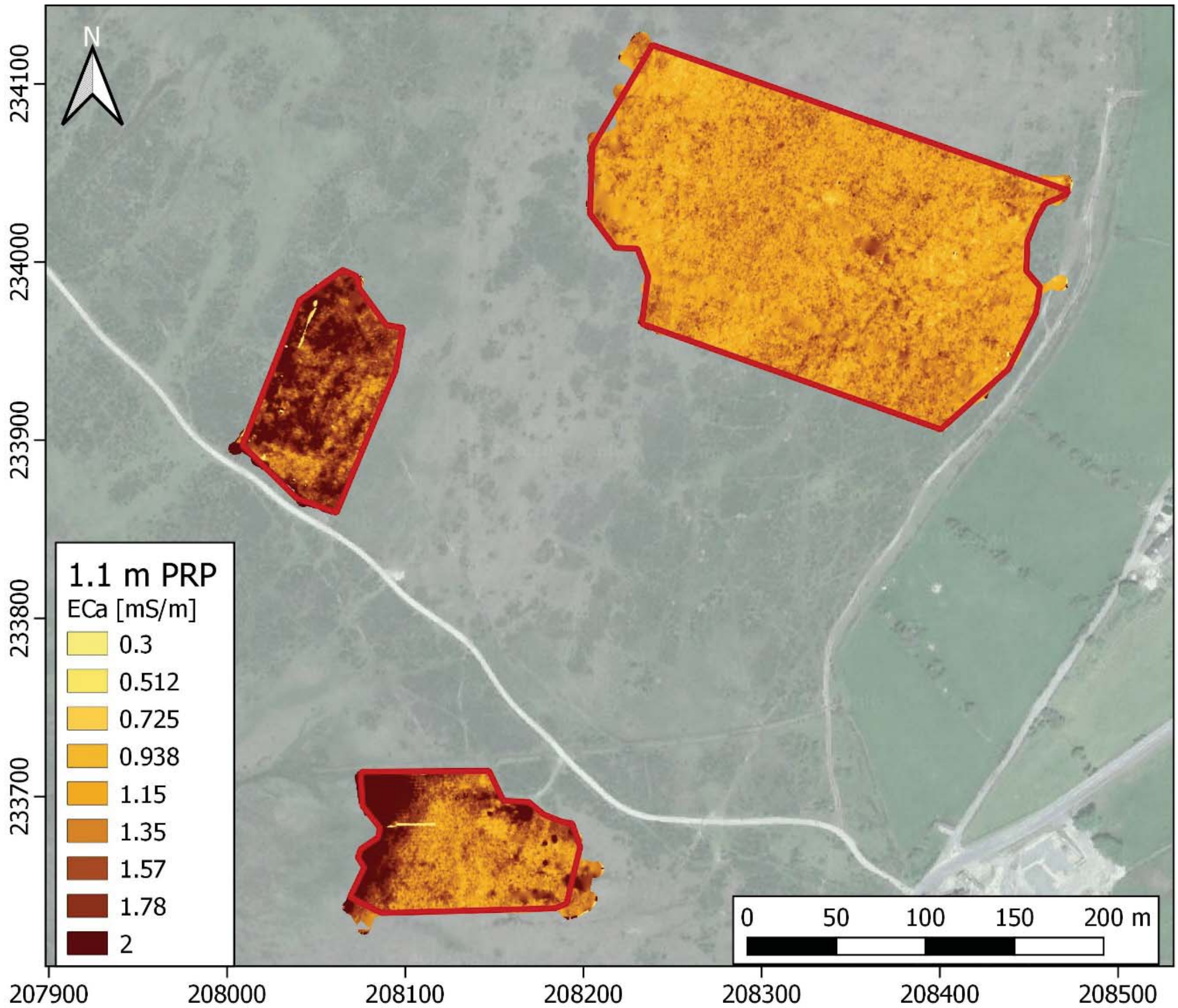

A 17: 1.1 m PRP - ECa data.

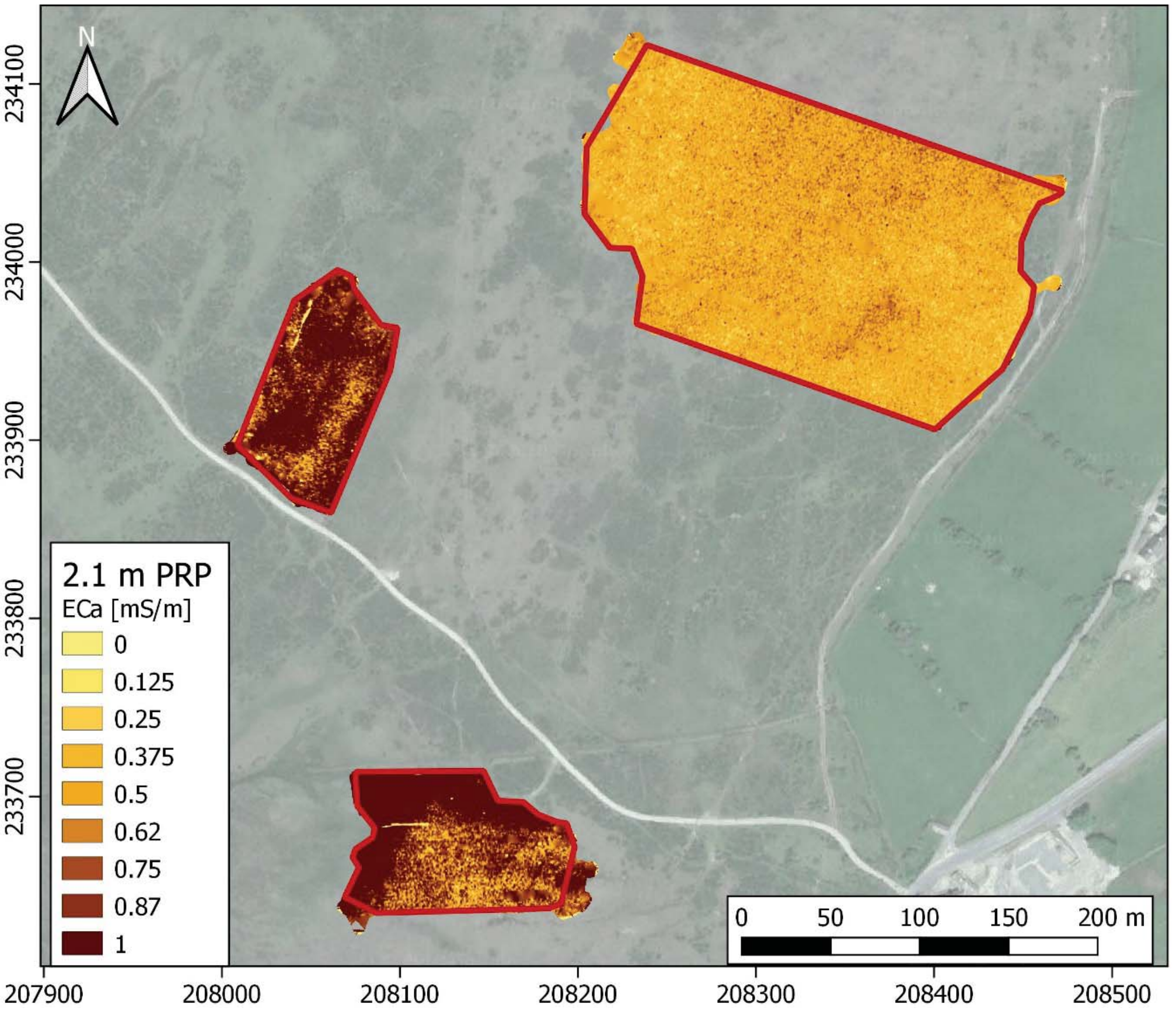

A 18: 2.1 m PRP - ECa data.

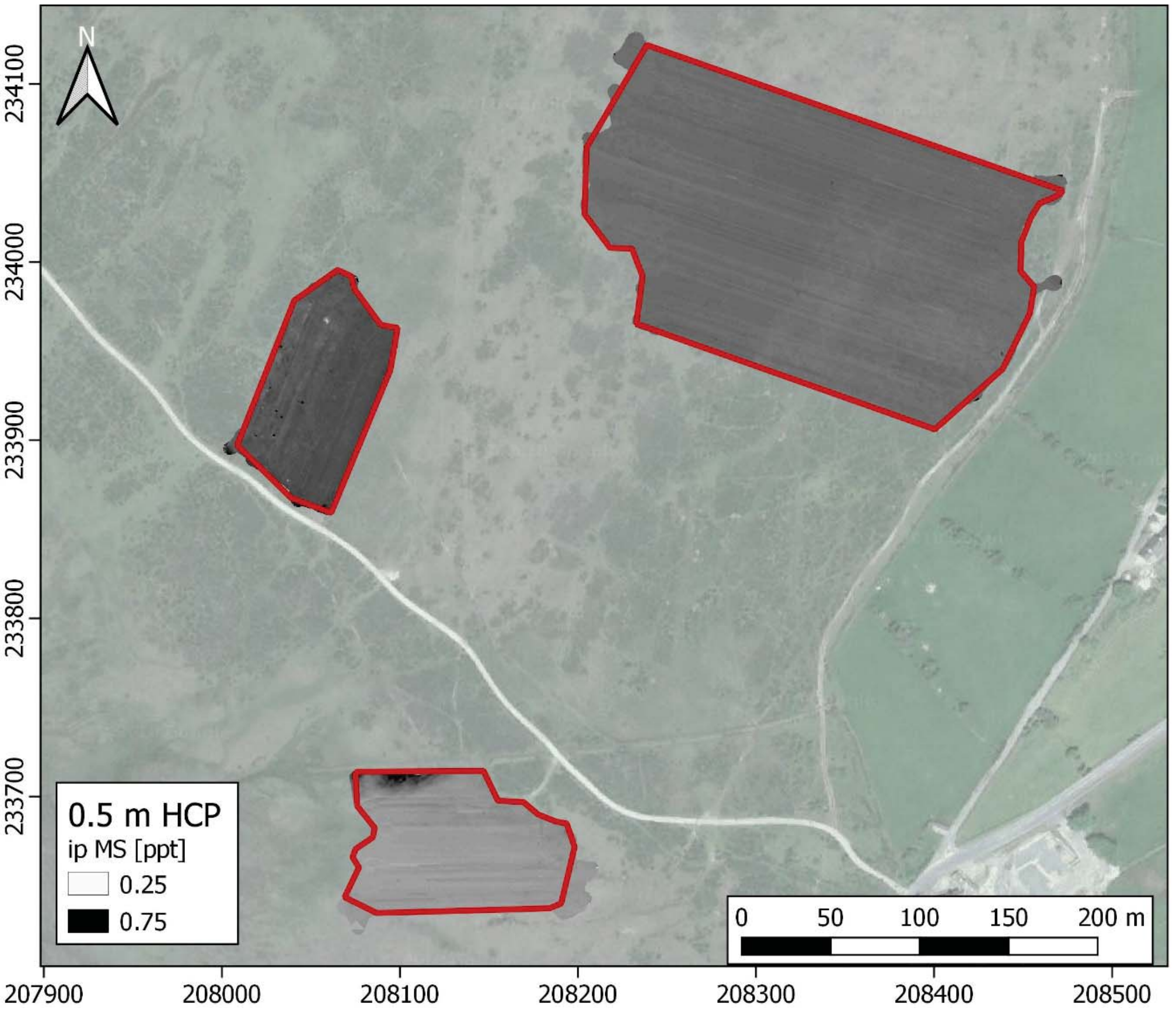

A 19: 0.5 m HCP - IP_MS data.

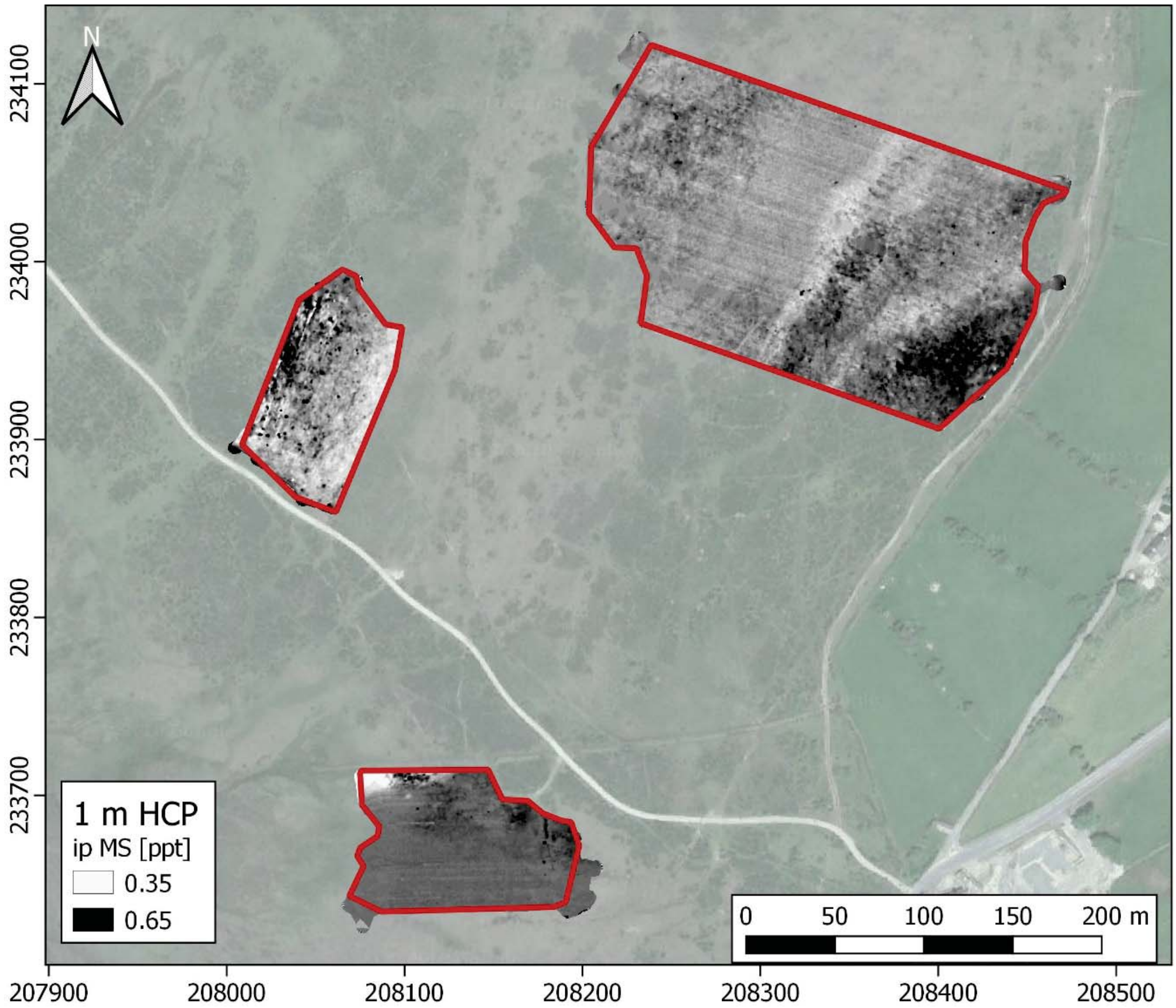

A 20: 1 m HCP - IP_MS data.

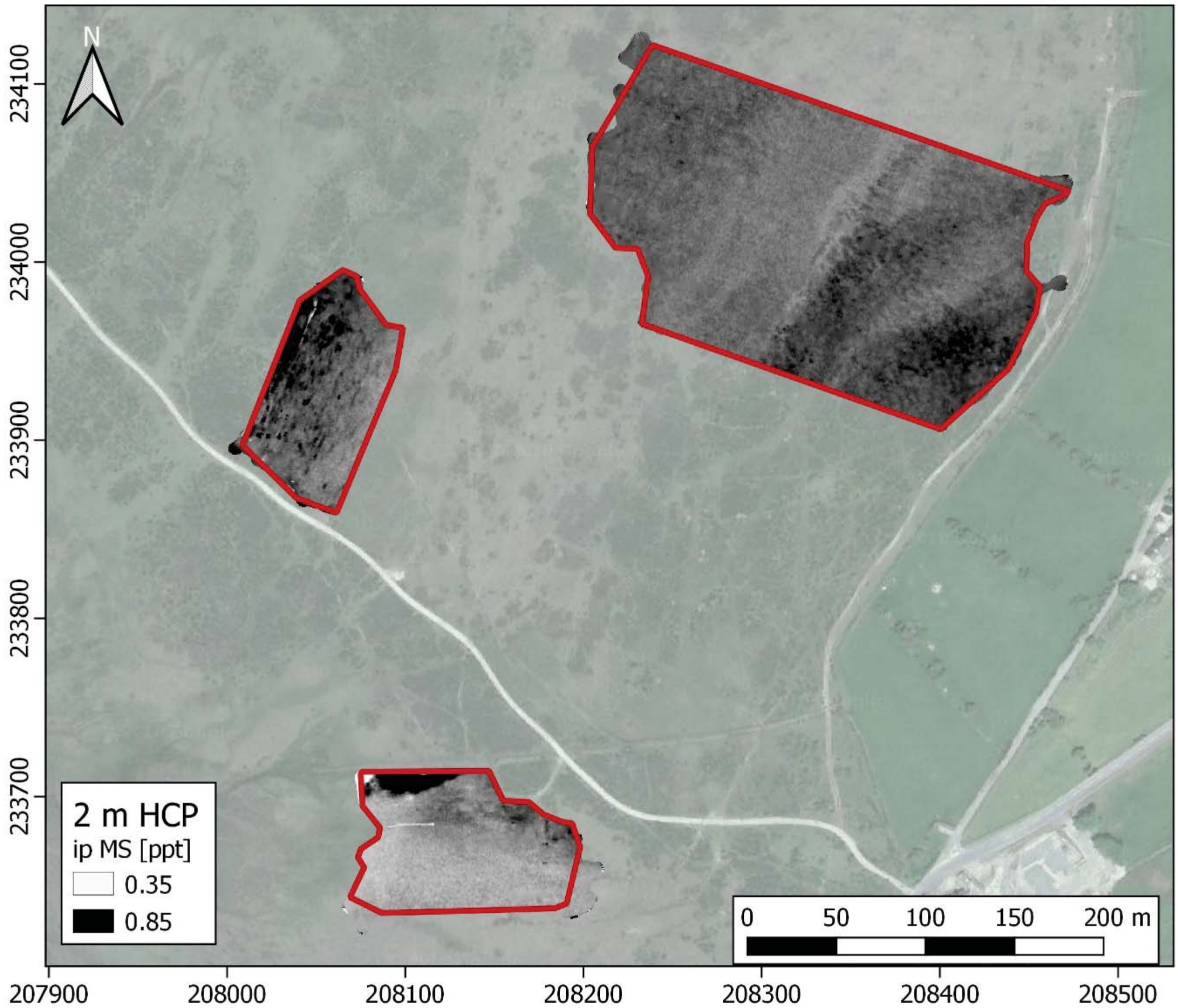

A 21: 2 m HCP - IP_MS data.

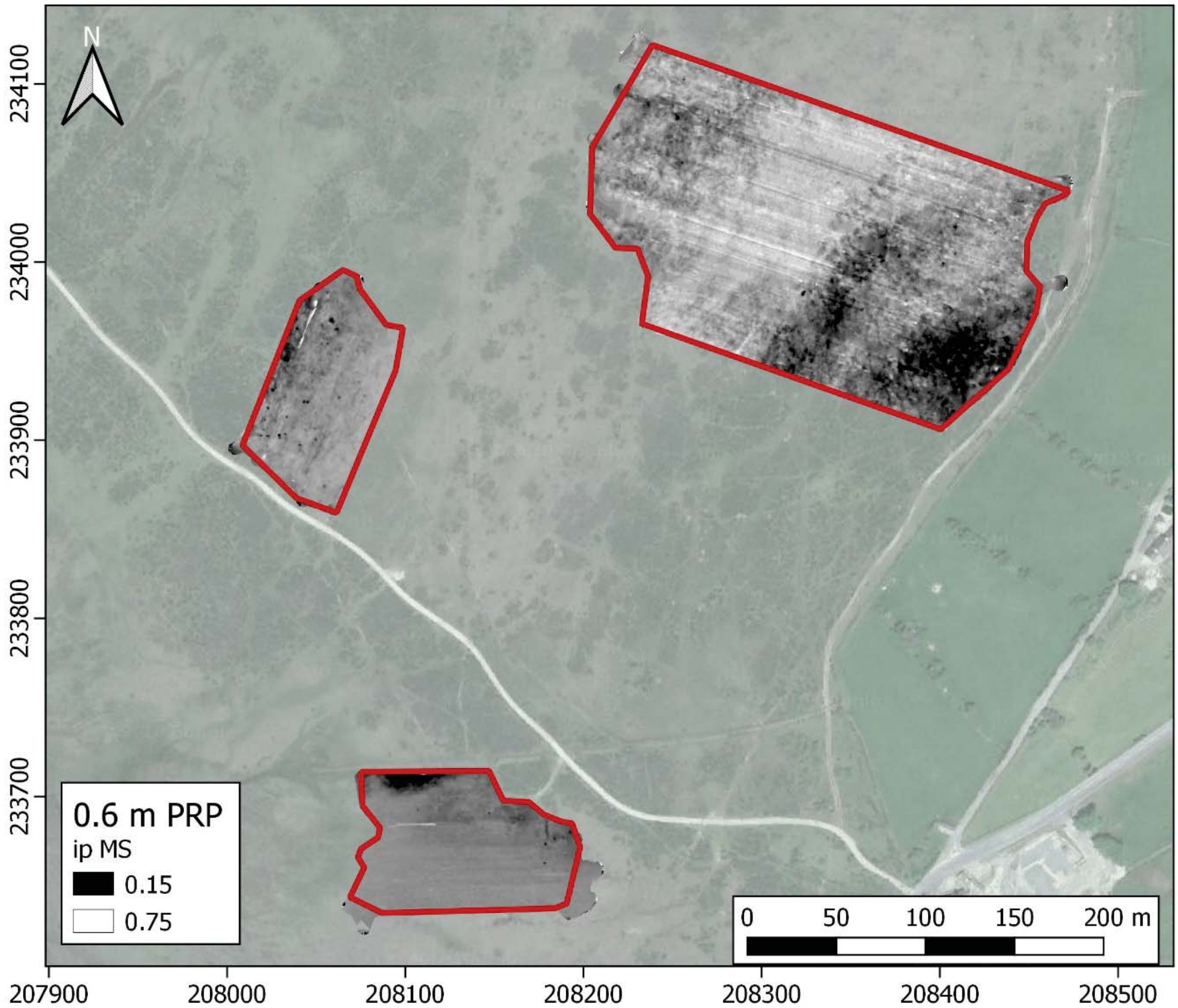

A 22: 0.6 m PRP - IP_MS data.

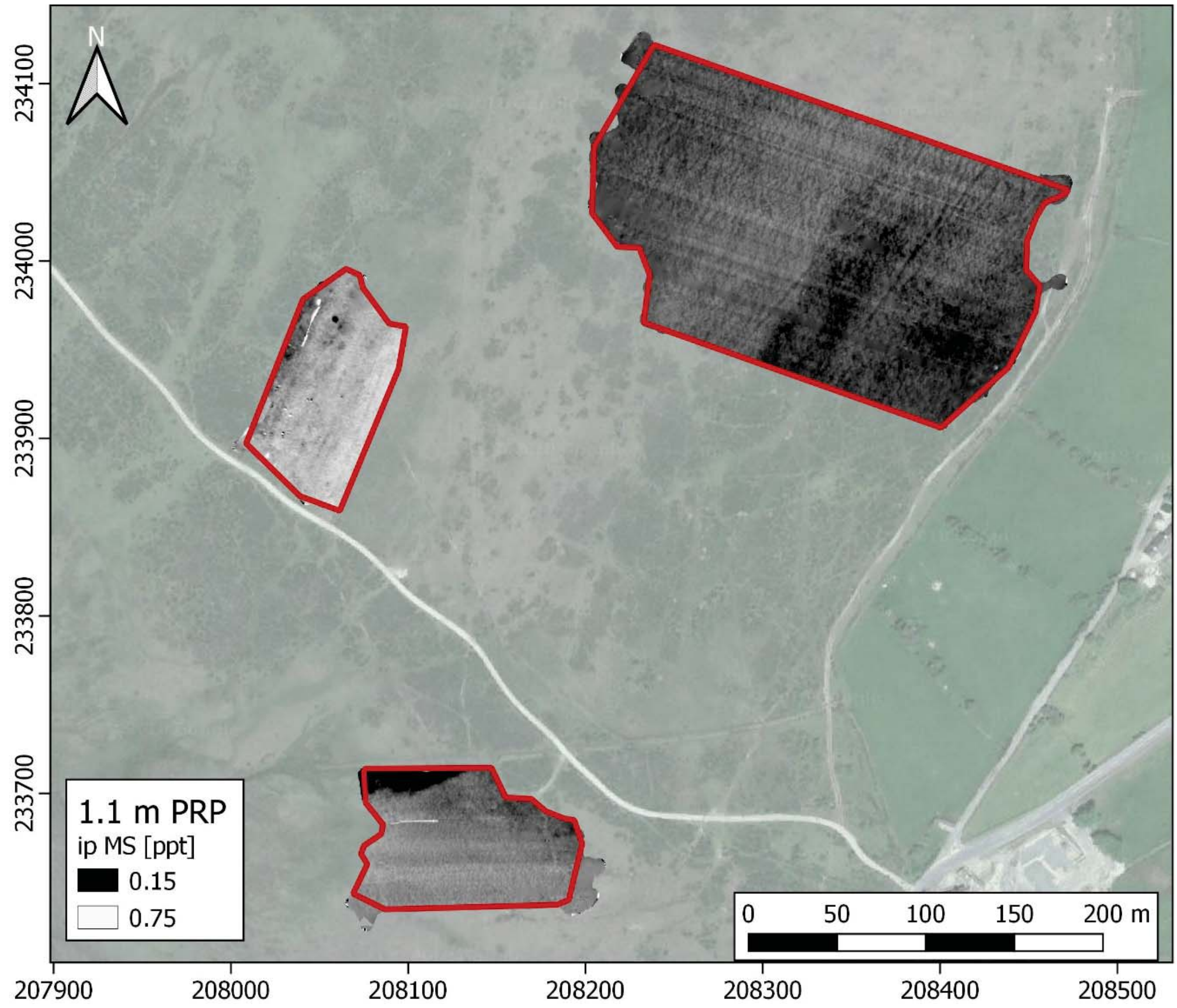

A 23: 1.1 m PRP - IP_MS data.

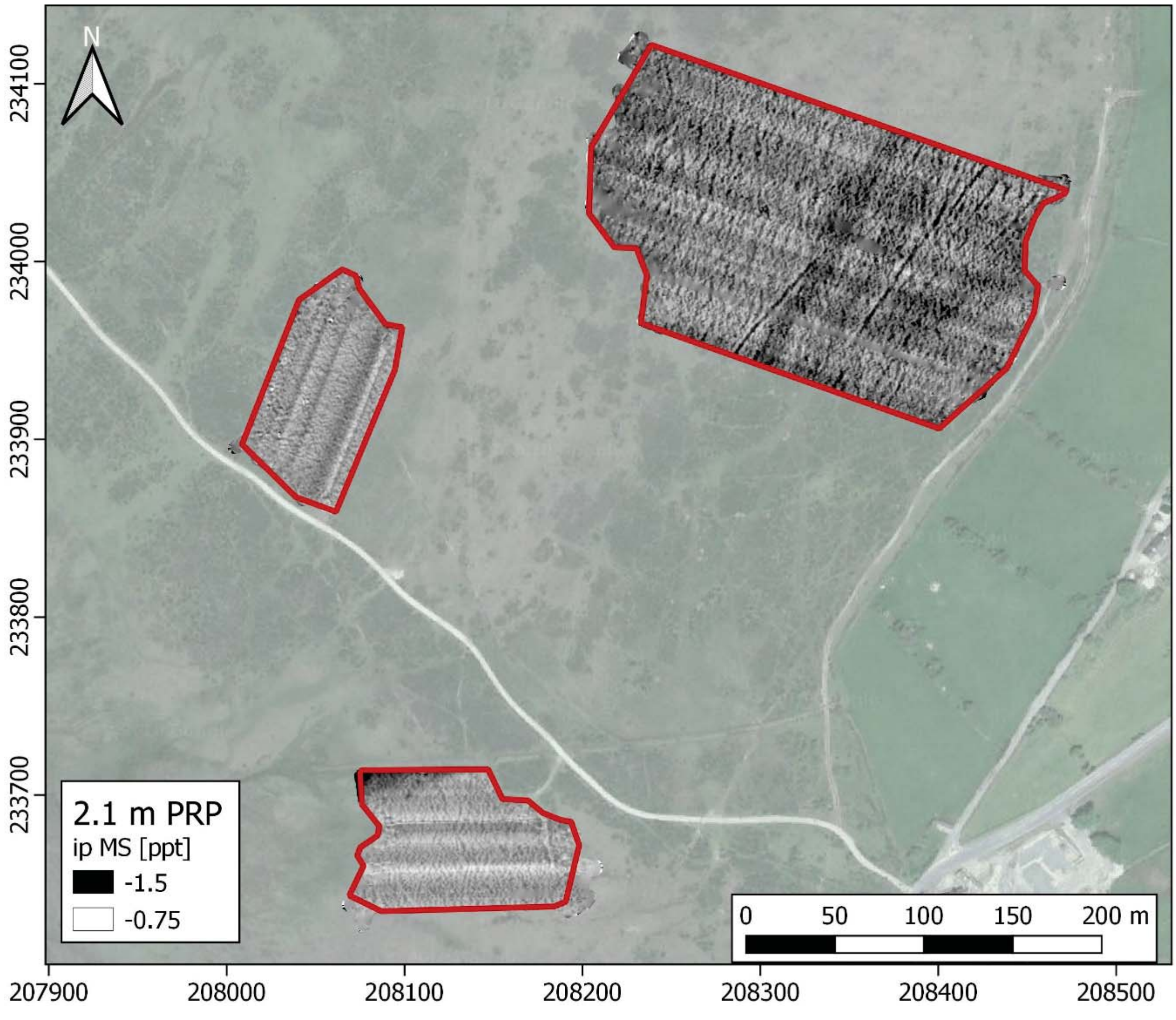

A 24: 2.1 m PRP - IP_MS data.

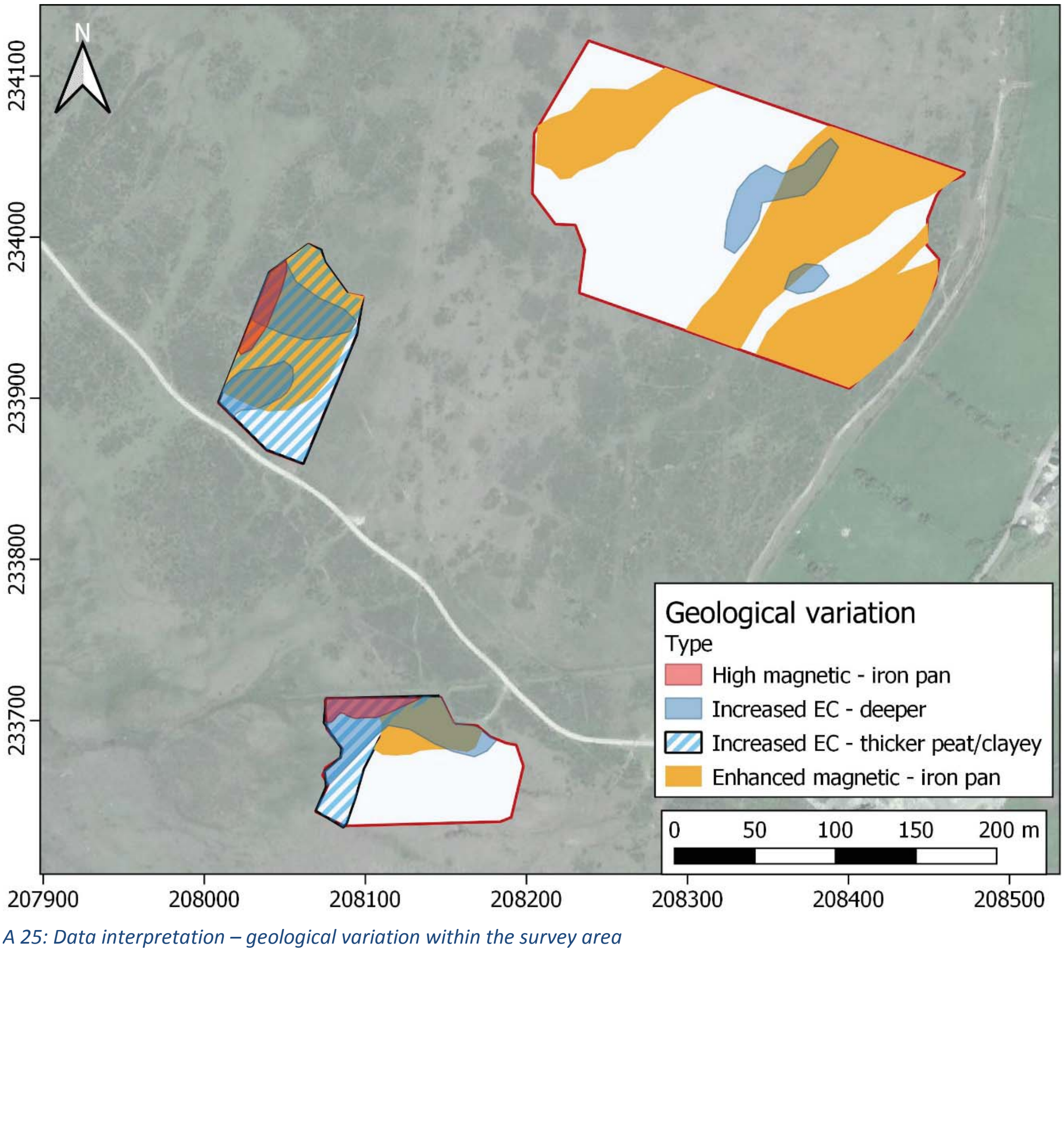

A 25: Data interpretation – geological variation within the survey area

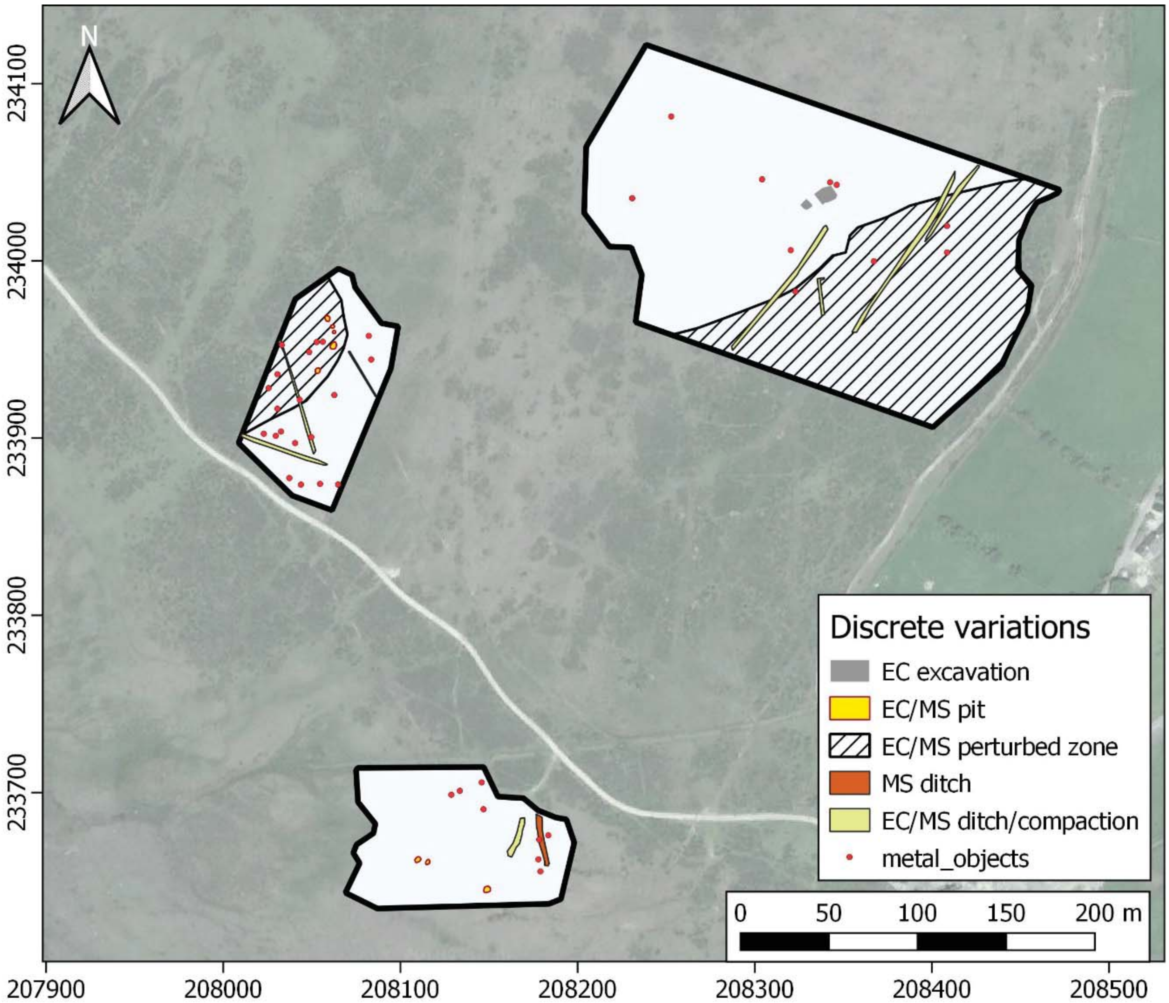

A 26: Data interpretation: small scale variation